



26 **KEYWORDS**

27 Prediction; rainfall and runoff; artificial neural network; modular model; singular  
28 spectrum analysis

29

30 **1. Introduction**

31 The rainfall-runoff relationship is one of the most complex hydrological  
32 phenomena to comprehend, owing to the tremendous spatial and temporal variability of  
33 watershed characteristics and precipitation patterns, and to the number of variables  
34 involved in the modeling of the physical process (Kumar et al., 2005). Since the rational  
35 method for peak of discharge was developed by Mulvany (1850), numerous hydrologic  
36 models have been proposed. Based on the description of the governing processes, these  
37 models can be classified as either physically-based (knowledge-driven) or system  
38 theoretic (data-driven). Physically-based models involve a detailed interaction of various  
39 physical processes controlling the hydrologic behavior of a system. However, system  
40 theoretic models are instead based primarily on observations (measured data) and seek to  
41 characterize the system response from those data using transfer functions. As an example  
42 of system theoretic models, ANN-based R-R models have received great attentions in the  
43 last two decades due to their capability to reproduce the highly nonlinear nature of the  
44 relationship between hydrological variables.

45 The potential of ANN in hydrological modeling was reviewed, for example, by the  
46 ASCE Task Committee on Application of the ANNs in hydrology (ASCE, 2000), Maier  
47 and Dandy (2000), and Dawson and Wilby (2001). Most applications for river flow  
48 prediction consist in modeling the R-R transformation, providing input of past flows and  
49 precipitation observations. They have proved that ANNs are able to outperform traditional  
50 statistical R-R modeling (Hsu et al, 1995; Shamseldin, 1997; Sajikumar and

51 Thandaveswara, 1999; Tokar and Johnson, 1999; Coulibaly et al., 2000; Sudheer et al.,  
52 2002) and to offer promising alternatives for conceptual R-R models (Hsu et al,  
53 1995; Tokar and Johnson, 1999; Coulibaly et al., 2000; Dibike and Solomatine,  
54 2001; Birikundavyi et al., 2002; de Vos and Rientjes, 2005; Toth and Brath, 2007). Hsu *et*  
55 *al.* (1995) showed that the ANN model provided a better representation of the rainfall-  
56 runoff relationships than the ARMAX time series model or the conceptual SAC-SMA  
57 (Sacramento soil moisture accounting) models. Coulibaly et al. (2000) used the early  
58 stopping method, to train multi-layer perceptrons (MLP) for real-time reservoir inflow  
59 prediction. Results show that MLP can provide better model performance compared to  
60 benchmarks from the classic autoregressive model coupled with a Kalman filter  
61 (ARMAX-KF) and a conceptual model (PREVIS). Birikundavyi et al. (2002) investigated  
62 the ANN models for daily streamflow prediction and also showed that ANNs  
63 outperformed PREVIS and ARMAX-KF. Toth and Brath (2007) investigated the impact  
64 of the amount of the training data on model performance using ANN and a conceptual  
65 model (ADM). ANN was proved to be an excellent tool for the R-R simulation of  
66 continuous periods, provided that an extensive set of hydro-meteorological data was  
67 available for calibration purposes. However, compared with ANN, ADM may allow a  
68 significant prediction improvement when focusing on the prediction of flood events and  
69 especially in case of a limited availability of the training data.

70 Improvement of model performance is a long-term topic of interest by researchers  
71 when ANN is used to simulate the R-R relationship. It is recognized that the ANN model  
72 is data dependent and has a flexible structure, which leaves huge room for the  
73 improvement of ANN in the context of R-R prediction. The ANN model is highly  
74 sensitive to the studied data, which means that the structure of ANN is totally different  
75 with the change of the training data. Besides, the training algorithms, model configuration,

76 and data preprocessing techniques also impose wide influences on the model performance.  
77 Hsu et al. (1995) found that the ANN models underestimated low flows and  
78 overestimated medium flows when they were used to simulate the R-R relationship. They  
79 further mentioned that this might have been due to the models not being able to capture  
80 the nonlinearity in the rainfall-runoff process and suggested that there is still room for  
81 improvement in applying different algorithms, such as stochastic global optimization and  
82 genetic algorithms, to reach near global solutions, and achieve better model performances.  
83 Hence, a more effective and efficient ANN R-R model was developed by Jain and  
84 Srinivasulu (2004) where ANN was trained by using real-coded GAs. Results showed that  
85 the proposed approach could significantly improve the estimation accuracy of the low-  
86 magnitude flows.

87 On the other hand, Zhang and Govindaraju (2000) recently pointed out that the  
88 rainfall-runoff mapping in a watershed can be fragmented or discontinuous with  
89 significant variations over the input space because of the functional relationships between  
90 rainfall and runoff being quite different for low, medium, and high magnitudes of  
91 streamflow. They found a single ANN to be rigid in nature and not suitable in capturing a  
92 fragmented input-output mapping. In order to overcome this problem they designed a  
93 modular neural network (MANN) consisting of three different ANN models for low-,  
94 medium-, and high-magnitude flows. Inspired by this study, many modular (or hybrid)  
95 models have been developed for R-R simulation. Solomatine and Xue (2004) applied an  
96 approach where separate ANN and M5 model-tree basin models were built for various  
97 hydrological regimes (identified on the basis of hydrological domain knowledge). Jain  
98 and Srinivasulu (2006) also applied decomposition of the flow hydrograph by a certain  
99 threshold value and then built separate ANNs for low and high flow regimes. Corzo and  
100 Solomatine (2007) investigated three modular ANNs for simulating two decomposed flow

101 regimes, base flow and exceeding flow, depending on three different partitioning schemes:  
102 automatic classification based on clustering, temporal segmentation of the hydrograph  
103 based on an adapted baseflow separation technique, and an optimized baseflow separation  
104 filter. The modular models were shown to be more accurate than the global ANN model.  
105 The best modular model was the one using the optimized baseflow filtering equation.  
106 Evidently, all studies demonstrated that modular models generally made higher accuracy  
107 of prediction than global models built to represent all possible regimes of the modeled  
108 system. Hence, MANN continues to be examined in the present study.

109         When a rainfall or runoff (streamflow or discharge) time series is viewed as a  
110 combination of quasi-periodic signals contaminated by noises to some extent, a cleaner  
111 time series can be filtered by appropriate data preprocessing techniques such as singular  
112 spectrum analysis (SSA). Obviously, the predictability of a system can be improved by  
113 predicting the important oscillations (periodic components) taken from the system. For  
114 the purpose of cleaning rainfall or runoff series, many data preprocessing techniques,  
115 including Moving average (MA), Principal component analysis (PCA), wavelet analysis  
116 (WA), and singular spectrum analysis (SSA), have been employed in hydrology field by  
117 researchers (Sivapragasam et al., 2001; Marques et al., 2006; Hu et al., 2007; Partal and  
118 Kişi, 2007; Sivapragasam et al., 2007; Wu et al., 2010). Hu et al. (2007) employed PCA  
119 as an input data preprocessing tool to improve the prediction accuracy of the rainfall-  
120 runoff neural network models. The use of WA to improve rainfall forecasting was  
121 conducted by Partal and Kişi (2007). Their results indicated that WA was promising. Wu  
122 et al. (2010) compared MA, PCA and SSA as data preprocessing methods using ANN for  
123 rainfall predictions and found that SSA is preferred. SSA has also been recognized as an  
124 efficient preprocessing algorithm to avoid the effect of discontinuous or intermittent  
125 signals, coupled with neural networks (or similar approaches) for time series forecasting

126 (Lisi et al., 1995; Sivapragasam et al., 2001; Baratta et al., 2003). For example, Lisi et al.  
127 (1995) applied SSA to extract the significant components in their study on southern  
128 oscillation index time series and used ANN for prediction. They reconstructed the original  
129 series by summing up the first “p” significant components. Sivapragasam et al. (2001)  
130 proposed a hybrid model of support vector machine (SVM) and SSA for rainfall and  
131 runoff predictions. The hybrid model resulted in a considerable improvement in the model  
132 performance in comparison with the original SVM model. However, few studies employ  
133 SSA to filter rainfall and streamflow so as to generate cleaner inputs for an R-R model.  
134 Therefore, one of main purposes in this study is to develop an ANN (or MANN) R-R  
135 model coupled with SSA. To evaluate its performance, a linear regression (LR) R-R  
136 model and an ANN-based time series model (using antecedent runoff as only input  
137 variables) are developed as benchmarks. To ensure wider applications of conclusions, two  
138 river basins from China, Wuxi and Luishui, are explored.

139 This paper is structured in the following manner. Followed by Introduction, the  
140 study areas are described and modeling methods are presented. Section 3 presents their  
141 applications to two watersheds. The optimal model is identified and the implementation  
142 of SSA is described. In Section 4, main results are shown along with necessary  
143 discussions. Section 5 summarizes main conclusions in this study.

## 144 **2. Methodology**

### 145 **2.1 Study Area and Data**

146 Two river basins from China, Daning and Lushui, are considered as case studies.

147 The Daning River, a first-order tributary of the Yangtze River, is located in the  
148 northeast of Chongqing city. The collected daily data includes rainfall, runoff (or  
149 streamflow), and evaporation. The data period spans 20 years from January 1, 1988 to  
150 December 31, 2007. The daily rainfall data are measured at six rain gauges located at the

151 upstream of the basin. The upstream part is controlled by “Wuxi” hydrology station, with  
152 a drainage area of around 2 000 km<sup>2</sup>. The data of runoff and evaporation are gathered at  
153 “Wuxi” station (hereafter the studied area is denoted by “Wuxi”). The Lushui River,  
154 located in the southeast of Hubei province, is also a first-order tributary of the Yangtze  
155 River. The collected daily data includes runoff and rainfall. The data period covers a 4-  
156 year long duration (January 1, 2004 - December 31, 2007). The runoff data from Lushui  
157 River are collected at “Chongyang” hydrology station. The daily rainfall data are  
158 measured at eight rain gauges located at the drainage area controlled by Chongyang  
159 hydrology station. The drainage area controlled by the station is around 1 700 km<sup>2</sup>  
160 (hereafter the studied area is referred to as “Chongyang”). Figure 1 demonstrates rainfall  
161 and runoff (or streamflow) time series in two basins. The data represents various types of  
162 hydrological conditions, and flow range from low to very high.

163         Each prediction model is a lumped type, namely, the watershed is considered as a  
164 whole, the input rainfall being the mean areal precipitation over the watershed by  
165 Thiessen polygon method and the output being the runoff measured at the control  
166 hydrology station. The entire input-output dataset in each watershed is partitioned into  
167 three data subsets as training set, cross-validation set and testing set: the first half of the  
168 entire data as training set and the first half of the remaining data as cross-validation set  
169 and the other half as testing set. The training set serves the model training and the testing  
170 set is used to evaluate the performances of models. The cross-validation set has dual  
171 functions: one is to implement an early stopping approach so as to avoid overfitting of the  
172 training data, and another is to select some best predictions from a large number of  
173 ANN’s runs. Ten best predictions are selected from twenty ANN’s runs in the present  
174 study. Moreover, ANN employs the hyperbolic tangent function as transfer functions in  
175 both hidden and output layers. Table 1 presents statistical information on rainfall and

176 streamflow data, including mean ( $\mu$ ), standard deviation ( $S_x$ ), coefficient of variation  
177 ( $C_v$ ), skewness coefficient ( $C_s$ ), minimum ( $X_{\min}$ ), and maximum ( $X_{\max}$ ). Obviously,  
178 the training data cannot fully include the cross-validation and testing data in terms of  
179 Wuxi. It's recommended that all data be scaled to the interval [-0.9, 0.9] instead of [-1, 1]  
180 which is the range of the hyperbolic tangent function. The advantage of using [-0.9, 0.9]  
181 is that some extreme data occurring outside the range of the training data may be  
182 accommodated in the mapping of ANN.

## 183 **2.2 Singular spectrum analysis**

184 According to Golyandina et al. (2001), the basic SSA consists of two stages:  
185 decomposition and reconstruction. The decomposition stage involves two steps:  
186 embedding and singular values decomposition (SVD); the reconstruction stage also  
187 comprises two steps: grouping and diagonal averaging. Consider a real-valued time series  
188  $F = \{x_1, x_2, \dots, x_N\}$  of length  $N (> 2)$ . Assume that the series is a nonzero series, viz. there  
189 exists at least one  $i$  such that  $x_i \neq 0$ . Four steps are briefly presented as follows.

### 190 ***1st step: embedding***

191 The embedding procedure maps the original time series to a sequence of multi-  
192 dimensional lagged vectors. Let  $L$  be an integer (window length),  $1 < L < N$ , and  $\tau$  be  
193 the delayed time as the multiple of the sampling period. The embedding procedure forms  
194  $n = N - (L - 1)\tau$  lagged vectors  $\mathbf{x}_i = \{x_i, x_{i+\tau}, x_{i+2\tau}, \dots, x_{i+(L-1)\tau}\}^T$ , where  $\mathbf{x}_i \in \mathbf{R}^L$ , and  
195  $i = 1, 2, \dots, n$ . The 'trajectory matrix' of the time series is denoted by  
196  $\mathbf{X} = [\mathbf{x}_1 \ \dots \ \mathbf{x}_i \ \dots \ \mathbf{x}_n]$  having lagged vectors as its columns. In other words, the  
197 trajectory matrix is



$$\mathbf{X} = \begin{pmatrix} x_1 & x_2 & x_3 & \dots & x_n \\ x_{1+\tau} & x_{2+\tau} & x_{3+\tau} & \dots & x_{n+\tau} \\ x_{1+2\tau} & x_{2+2\tau} & x_{3+2\tau} & \dots & x_{n+2\tau} \\ \vdots & \vdots & \vdots & \vdots & \vdots \\ x_{1+(L-1)\tau} & x_{2+(L-1)\tau} & x_{3+(L-1)\tau} & \dots & x_N \end{pmatrix} \quad (1)$$

199 If  $\tau = 1$ , the matrix  $\mathbf{X}$  is called Hankel matrix since it has equal elements on the  
 200 ‘diagonals’ where the sum of subscripts of row and column is equal to a constant. If  $\tau > 1$ ,  
 201 the equal elements in  $\mathbf{X}$  are not definitely in the ‘diagonals’.

202 **2nd step: SVD**

203 Let  $\mathbf{S} = \mathbf{X}\mathbf{X}^T$ . Denoted by  $\lambda_1, \lambda_2, \dots, \lambda_L$  the eigenvalues of  $\mathbf{S}$  taken in the  
 204 decreasing order of magnitude ( $\lambda_1 \geq \lambda_2 \geq \dots \geq \lambda_L \geq 0$ ) and by  $\mathbf{u}_1, \mathbf{u}_2, \dots, \mathbf{u}_L$  the  
 205 orthonormal system of the eigenvectors of the matrix  $\mathbf{S}$  corresponding to these  
 206 eigenvalues. If we denote  $\mathbf{v}_i = \mathbf{X}_i^T \mathbf{u}_i / \sqrt{\lambda_i}$  ( $i = 1, \dots, L$ ) (equivalent to the  $i$ th eigenvector of  
 207  $\mathbf{X}^T \mathbf{X}$ ), then the SVD of the trajectory matrix  $\mathbf{X}$  can be written as

$$\mathbf{X} = \mathbf{X}_1 + \dots + \mathbf{X}_L \quad (2)$$

209 where  $\mathbf{X}_i = \sqrt{\lambda_i} \mathbf{u}_i \mathbf{v}_i^T$ . The matrices  $\mathbf{X}_i$  have rank 1; therefore they are elementary matrices.  
 210 The collection  $(\lambda_i, \mathbf{u}_i, \mathbf{v}_i)$  will be called  $i$ th eigentriple of the SVD. Note that  $\mathbf{u}_i$  and  $\mathbf{v}_i$   
 211 are also  $i$ th left and right singular vectors of  $\mathbf{X}$ , respectively.

212 **3rd step: grouping**

213 The purpose of this step is to appropriately identify the trend component,  
 214 oscillatory components with different periods, and structureless noises by grouping  
 215 components. This step can be also skipped if one does not want to precisely extract  
 216 hidden information by regrouping and filter of components.

217 The grouping procedure partitions the set of indices  $\{1, \dots, L\}$  into  $m$  disjoint  
 218 subsets  $I_1, \dots, I_m$ , so the elementary matrix in Eq. (2) is regrouped into  $m$  groups. Let

219  $I = \{i_1, \dots, i_p\}$ . Then the resultant matrix  $\mathbf{X}_I$  corresponding to the group  $I$  is defined as

220  $\mathbf{X}_I = \mathbf{X}_{i_1} + \dots + \mathbf{X}_{i_p}$ . These matrices are computed for  $I_1, \dots, I_m$  and substituting into Eq. (2)

221 one obtains the new expansion

$$222 \quad \mathbf{X} = \mathbf{X}_{I_1} + \dots + \mathbf{X}_{I_m} \quad (3)$$

223 The procedure of choosing the sets  $I_1, \dots, I_m$  is called the eigentriple grouping.

224 **4th step: Diagonal averaging**

225 The last step in the Basis SSA transforms each resultant matrix of the grouped

226 decomposition (3) into a new series of length  $N$ . The diagonal averaging is to find equal

227 elements in the resultant matrix and then to generate a new element by averaging over

228 them. The new element has the same position (or index) as that of these equal elements in

229 the original series. As mentioned in the step 1, the concept of ‘diagonal’ is not true for

230  $\tau > 1$ . Regardless of the value of  $\tau$  larger than or equal 1, the principle of reconstruction

231 is the same. For  $\tau = 1$ , the diagonal averaging can be carried out by formula

232 recommended by Golyandina et al. (2001). Let  $\mathbf{Y}$  be a  $(L \times n)$  matrix with elements  $y_{ij}$ ,

233  $1 \leq i \leq L$ ,  $1 \leq j \leq n$ . Make  $L^* = \min(L, n)$ ,  $n^* = \max(L, n)$  and  $N = n + (L - 1)\tau$ . Let

234  $y_{ij}^* = y_{ij}$  if  $L < n$  and  $y_{ij}^* = y_{ji}$  otherwise. Diagonal averaging transfers matrix  $\mathbf{Y}$  to a

235 series  $\{y_1, y_2, \dots, y_N\}$  by the following equation:

$$236 \quad y_k = \begin{cases} \frac{1}{k} \sum_{m=1}^k y_{m, k-m+1}^* & \text{for } 1 \leq k < L^* \\ \frac{1}{L^*} \sum_{m=1}^{L^*} y_{m, k-m+1}^* & \text{for } L^* \leq k \leq K^* \\ \frac{1}{N-k+1} \sum_{m=k-K^*+1}^{N-K^*+1} y_{m, k-m+1}^* & \text{for } L^* < k \leq N \end{cases} \quad (4)$$

237 Eq. (4) corresponds to averaging of the matrix elements over the ‘diagonals’  $i + j = k + 1$ .

238 The diagonal averaging, applied to a resultant matrix  $\mathbf{X}_k$ , produces a  $N$  – length series  $F_k$ ,

239 and thus the original series  $F$  is decomposed into the sum of  $m$  series:

240 
$$F = F_1 + \dots + F_m \quad (5)$$

241 As mentioned above, these reconstructed components (RCs) can be associated with the

242 trend, oscillations or noise of the original time series with proper choices of  $L$  and the sets

243 of  $I_1, \dots, I_m$ . Certainly, if the third step (namely, grouping) is skipped,  $F$  can be

244 decomposed into  $L$  RCs.

### 245 **2.3 Model development**

246 A representative data-driven R-R model can be defined as

247 
$$\hat{Q}_{t+T} = f(\mathbf{X}_t) = f(Q_{t+1-l_1}, R_{t+1-l_2}, S_{t+1-l_3}) \quad (6)$$

248 where  $\hat{Q}_{t+T}$  stands for the predicted flow at time instance  $t + T$ ;  $T$  (with  $T = 1, 2, 3$  for the

249 present study) refers to how far into the future the runoff prediction is desired;  $Q_{t+1-l_1}$  is

250 the antecedent flow (up to  $t + 1 - l_1$  time steps),  $R_{t+1-l_2}$  is the antecedent rainfall (up to

251  $t + 1 - l_2$  time steps) and  $S_{t+1-l_3}$  ( up to  $t + 1 - l_3$  time steps) represents any other factors

252 contributing to the true flow  $Q_{t+T}$ , such as evaporation or temperature;  $l_1$ ,  $l_2$ , and  $l_3$

253 respectively stand for the number of previous flow, rainfall and other factors. The

254 predictability of future behavior is a consequence of the correct identification of the

255 system transfer function of  $f(\bullet)$ . Herein, linear regression and nonlinear regression (e.g.

256 ANN) techniques are respectively used to approximate the  $f(\bullet)$ .

#### 257 **(1) LR**

258 The LR model herein is actually called stepwise linear regression (SLR) model

259 because the forward stepwise regression is used to determine optimal input variables. The

260 basic idea of SLR is to start with a function that contains the single best input variable and  
261 to subsequently add potential input variables to the function one at a time in an attempt to  
262 improve model performance. The order of addition is determined by using the partial  
263  $F$ -test values to select which variable should enter next. The high partial  $F$ -value is  
264 compared to a (select or default)  $F$ -to-enter value. After a variable has been added, the  
265 function is examined to see if any variable should be deleted. More details can be found  
266 in Draper and Smith (1998) and McCuen (2005).

## 267 (2) ANN

268 The multilayer perceptron network is by far, among ANN paradigms, the most  
269 popular, which usually uses the technique of error back propagation to train the network  
270 configuration. The architecture of the ANN consists of a number of hidden layers and a  
271 number of neurons in the input layer, hidden layers and output layer. ANNs with one  
272 hidden layer are commonly used in hydrologic modeling (Dawson and Wilby, 2001; de  
273 Vos and Rientjes, 2005) since these networks are considered to provide enough  
274 complexity to accurately simulate the nonlinear-properties of the hydrologic process. The  
275 three-layer ANN can be denoted by  $m \times h \times 1$  where  $m$  stands for number of neuron in the  
276 input layer and  $h$  is the number of neuron in the hidden layer. According to Eq. (6),  
277  $m = l_1 + l_2 + l_3$ . The ANN prediction model is formulated as

$$278 \quad \hat{Q}_{t+T} = f(\mathbf{X}_t, w, \theta, m, h) = \theta_0 + \sum_{j=1}^h w_j^{out} \varphi\left(\sum_{i=1}^m w_{ji} \mathbf{X}_t + \theta_j\right) \quad (7)$$

279 where  $\varphi$  denotes transfer functions;  $w_{ji}$  are the weights defining the link between the  $i$ th  
280 node of the input layer and the  $j$ th of the hidden layer;  $\theta_j$  are biases associated to the  
281  $j$ th node of the hidden layer;  $w_j^{out}$  are the weights associated to the connection between  
282 the  $j$ th node of the hidden layer and the node of the output layer; and  $\theta_0$  is the bias at the

283 output node. To apply Eq. (7) to runoff predictions, appropriate training algorithm is  
284 required to optimize  $w$  and  $\theta$ .

### 285 **(3) MANN**

286 To construct MANN, the training data have to be divided into several clusters  
287 according to cluster analysis techniques, and then each single model is applied to each  
288 cluster. The fuzzy c-means (FCM) clustering technique is adopted in the present study  
289 (e.g., Bezdek, 1981, Wang et al., 2006). It is able to generate either soft or crisp clusters.  
290 Predictions from a modular model can be conducted in two ways: soft and hard. Soft  
291 prediction means that the testing data can belong to each cluster with different weights.  
292 As a consequence, the modular model output would be a weighted average of the outputs  
293 of several single models fitted for each cluster of training data. Hard prediction is that the  
294 modular model output is directly from the output of only triggered local model. ANN (or  
295 similar techniques) is unable to extrapolate beyond the range of the data used for training.  
296 Otherwise, poor predictions or predictions can be expected when a new input data is  
297 outside the range of those used for training. Hard prediction method is, therefore, adopted  
298 in this study.

299 Figure 2 displays the schematic diagram of MANN where the training data is  
300 partitioned into three clusters. Once input-output pairs are obtained, they are first split  
301 into three subsets by the FCM technique, and then each subset is approximated by a single  
302 ANN. The final output of the modular model results directly from the output of one of  
303 three local models.

### 304 **2.4 Implementation framework of R-R prediction**

305 Figure 3 illustrates the implementation framework of rainfall-runoff prediction  
306 where four prediction models can be conducted in two modes: without/with three data  
307 preprocessing methods (dashed box). These acronyms in the column of “methods for

308 model inputs” represent five methods to determine model inputs: LCA (linear correlation  
309 analysis, Sudheer et al., 2002), AMI (average mutual information, Fraser and Swinney,  
310 1986), PMI (partial mutual information, May et al., 2008), SLR (stepwise linear  
311 regression), and MOGA (ANN based on multi-objective genetic algorithm, Giustolisi and  
312 Simeone, 2006).

## 313 **2.5 Evaluation of model performances**

314 The Pearson’s correlation coefficient ( $r$ ) or the coefficient of determination ( $R^2 =$   
315  $r^2$ ), have been identified as inappropriate measures in hydrologic model evaluation by  
316 Legates and McCabe (1999). The coefficient of efficiency (CE) (Nash and Sutcliffe, 1970)  
317 is a good alternative to  $r$  or  $R^2$  as a “goodness-of-fit” or relative error measure in that it is  
318 sensitive to differences in the observed and predicted means and variances. Legates and  
319 McCabe (1999) also suggested that a complete assessment of model performance should  
320 include at least one absolute error measure (e.g., RMSE) as necessary supplement to a  
321 relative error measure. Besides, the Persistence Index (PI) (Kitanidis And Bras, 1980) was  
322 adopted here for the purpose of checking the prediction lag effect. Three measures are  
323 therefore used in this study. They are listed below.

$$324 \quad CE = 1 - \frac{\sum_{i=1}^n (Q_i - \hat{Q}_i)^2}{\sum_{i=1}^n (Q_i - \bar{Q})^2} \quad (8)$$

$$325 \quad RMSE = \sqrt{\frac{1}{n} \sum_{i=1}^n (Q_i - \hat{Q}_i)^2} \quad (9)$$

$$326 \quad PI = 1 - \frac{\sum_{i=1}^n (Q_i - \hat{Q}_i)^2}{\sum_{i=1}^n (Q_i - Q_{i-1})^2} \quad (10)$$

327 In these equations,  $n$  is the number of observations,  $\hat{Q}_i$  stands for predicted flow,  $Q_i$   
328 represents observed flow,  $\bar{Q}$  denotes average observed flow, and  $Q_{i-1}$  is the flow estimate  
329 from a persistence model (or termed naïve model) that basically takes the last flow

330 observation (at time  $i$  minus the lead time  $l$ ) as the prediction. CE and PI values of 1  
331 stands for perfect fits. A small value of PI may imply the occurrence of the lag prediction.

### 332 **3. Applications of Models**

#### 333 **3.1 Potential input variables**

334 In the process of determining model inputs, the first step is to find out appropriate  
335 input variables (causal variables) for Eq. (6). In general, causal variables in the R-R  
336 relationship can be rainfall (precipitation), previous flows, evaporation, temperature etc.  
337 Depending on the availability of data, the input variables tend to be varied in previous  
338 studies. Most studies employed rainfall and previous flow (or water level) as inputs  
339 (Campolo et al., 1999; Liang et al., 2002; Xu and Li, 2002; Sivapragasam et al., 2007)  
340 whereas input variables in some studies also included additional factors such as  
341 temperature or evaporation (Abrahart et al., 1999; Tokar and Johnson, 1999; Zealand et al,  
342 1999; Zhang and Govindaraju, 2000; Coulibaly et al., 2001; Abebe and Price,  
343 2003; Solomatine and Dulal, 2003; Wilby et al., 2003; Hu et al., 2007; Toth and Brath,  
344 2007; Solomatine and Shrestha, 2009).

345 The necessity of previous flows in model inputs was widely recognized by  
346 researchers (Campolo et al., 1999; de Vos and Rientjes, 2005). Campolo et al. (1999)  
347 made use of distributed rainfall data observed at different raingauge stations for the  
348 prediction of water levels at the catchment outlet. Poor predicted results were achieved  
349 when only water levels were used as input. However, the accuracies of predictions were  
350 improved when rainfall and previous water levels were included in inputs. de Vos and  
351 Rientjes (2005) employed different model inputs as hydrological state representation of  
352 ANN. Results also showed that the ANN model with rainfall input variable only had the  
353 worst performance compared to those whose input variables consisting of rainfall, flow  
354 and/or other states.

355           However, some studies pointed out that evaporation (or temperature) as input  
356 variable seemed to be unnecessary (Abrahart et al., 2001; Anctil et al., 2004; Toth and  
357 Brath, 2007). Anctil et al. (2004) found that potential evapotranspiration failed to improve  
358 the MLP performance when it was introduced into the initial model inputs consisting of  
359 rainfall and streamflow for R-R modeling. Results from Toth and Brath (2007) also  
360 indicated that the inclusion of potential evapotranspiration values in inputs did not  
361 improve the prediction results, but gave rise to a slight deterioration in comparison with  
362 the use of precipitation data alone. That result may be explained by the fact that the  
363 addition of evapotranspiration (or temperature measures) input nodes increases the  
364 network complexity, and therefore the risk of overfitting. In the present experiments,  
365 analyses of LCA, AMI, and PMI between evaporation and streamflow indicate that  
366 evaporation can be excluded since the dependence relation is not significant. Therefore,  
367 rainfall and streamflow are identified as final input variables.

### 368 **3.2 Selection of model inputs**

369           Having chosen appropriate input variables, the next step is the determination of  
370 appropriate lags for each variable to form model inputs. ANN, equipped with Levenberg-  
371 Marquardt training algorithm and hyperbolic tangent transfer functions, is used as the  
372 benchmark model to examine five input methods.

373           Figure 4 demonstrates the results of LCA of the runoff series for Wuxi and  
374 Chongyang. The partial auto-correlation function (PACF) value decayed within the  
375 confidence band around at lag 5 for Wuxi and lag 4 for Chongyang. Therefore, the  
376 number  $l_1$  of lags of flow was initially set at the value of 5 for Wuxi and 4 for  
377 Chongyang. The number  $l_2$  of lags of rainfall is generally determined according to time  
378 of concentration of the watershed. The time of concentration used herein is estimated  
379 between the center of hyetograph and the peak flow. The average time of concentration is



380 approximately 1 day for Wuxi and Chongyang. To take account of delay between rainfall  
381 and runoff, the value of  $l_2$  is originally set to 5 for both Wuxi and Chongyang. Table 2  
382 presents the results of ANN with different model inputs determined by LCA, AMI, PMI,  
383 SLR and MOGA. These results are based on one-step-ahead flow prediction (i.e.  $\hat{Q}_{t+1}$   
384 where  $t$  represents the present time instance). In terms of RMSE, there is no salient  
385 difference among all five methods. However, our experiments reveal that the ANN with  
386 inputs from LCA outperforms the others in the SSA scenario. Moreover, LCA can  
387 significantly reduce the effort and computational time requirement in developing an ANN  
388 model. The LCA method is therefore adopted for the later analysis. Figure 5 illustrates  
389 cross correlation functions (CCFs) between rainfall and streamflow for Wuxi and  
390 Chongyang. The past five rainfall observations have significant relations (correlation  
391 coefficient  $> 0.2$ ) with the present streamflow. The most significant correlation occurs at  
392 the first lag which indicates the time of response of watershed being about 1 day.

393

### 394 **3.3 Identification of models**

395 The model identification of a prediction model is to determine the structure by  
396 using training data to optimize relevant model parameters once model inputs are already  
397 obtained.

#### 398 **(1) LR**

399 LR can be viewed as a model-driven model which has known model structure.  
400 Model identification only consists in optimizing the coefficient of each input. The  
401 stepwise linear regression (SLR) technique was used to concurrently determine the model  
402 inputs and the corresponding coefficients. With model inputs already obtained by SLR in  
403 Table 2, the LR model at one-step lead for Wuxi and Chongyang can expressed  
404 respectively as Eq. (11),

405 
$$\hat{Q}_{t+1} = -0.019Q_{t-4} + 0.025Q_{t-2} + 0.016Q_{t-1} + 0.469Q_t + 0.046R_{t-4} +$$
  
406 
$$0.07R_{t-3} + 0.027R_{t-2} + 0.121R_{t-1} + 0.272R_t$$
 (11)

406 and Eq. (12),

407 
$$\hat{Q}_{t+1} = 0.032Q_{t-3} + 0.526Q_t + 0.099R_{t-3} + 0.053R_{t-2} + 0.037R_{t-1} + 0.454R_t$$
 (12)

## 408 (2) ANN and MANN

409 As a three-layer MLP was adopted, the identification of ANN's structure is to  
410 optimize the number of hidden nodes  $h$  in the hidden layer when the model inputs have  
411 been determined by LCA and there is a unique model output. The optimal size  $h$  of the  
412 hidden layer is found by systematically increasing the number of hidden neurons from 1  
413 to 10 until the network performance on the cross-validation set no longer improves  
414 significantly. The identified configurations of ANN were 10-8-1 for Wuxi and 9-9-1 for  
415 Chongyang, respectively (presented in Table 2). The same method is used to identify  
416 three local ANNs in MANN. As a consequence, the structures of MANN are 10-4/4/2-1  
417 for Wuxi and 9-3/3/1-1 for Chongyang, respectively.

418 In order to perform multi-step-ahead predictions, two methods are available: (1)  
419 re-using a one-step-ahead prediction as input into the network, after which it predicts the  
420 two-step-ahead prediction, and so forth, and (2) by directly having the multi-step-ahead  
421 prediction as output. The former and the latter are respectively termed the dynamic model  
422 and static model. For simplification, the static model is adopted herein.

## 423 3.4 Decomposition of rainfall and runoff series by SSA

424 To filter raw rainfall and runoff series, each series needs to be decomposed into  
425 components with the aid of SSA. The decomposition by SSA requires identifying the  
426 parameter pair  $(\tau, L)$ . The choice of  $L$  represents a compromise between information  
427 content and statistical confidence (Elsner and Tsonis, 1996). The value of an appropriate  
428  $L$  should be able to clearly resolve different oscillations hidden in the original signal.

429 However, the present study does not require accurately resolving the raw rainfall signal  
430 into trends, oscillations, and noises. A rough resolution can be adequate for the separation  
431 of signals and noises where some leading eigenvalues should be identified. To select  $L$ , a  
432 small interval of [3, 10] was examined in the present study.

433 A target  $L$  can be empirically determined in accordance with a specified criterion:  
434 the singular spectrum under the target  $L$  can be distinguished markedly, i.e. singular  
435 values forming the singular spectrum are quite different from each other. Figure 6  
436 illustrates the sensitivity analysis of the singular spectrum on  $L$  for rainfall and  
437 streamflow series from two basins of Wuxi and Chongyang. Singular values of both  
438 rainfall and flow series in the Wuxi watershed are clearly separated. Clearly, in terms of  
439 the criterion,  $L$  can be arbitrarily chosen from 3 to 10. To obtain a more robust ANN  
440 model, it is recommended that a larger  $L$  be taken which results in more combinations of  
441 RCs in the process of seeking the optimal model inputs. Thus, the final  $L$  is set at the  
442 value of 9 for the Wuxi rainfall, 7 for the Wuxi flow, 7 for both Chongyang rainfall and  
443 flow. Figure 6 highlights the singular spectrum curve associated with the selected  $L$  in  
444 the dotted line.

445 Figure 7 shows the results of sensitivity analysis of the singular spectrum on the  
446 lag time  $\tau$  using SSA with the chosen  $L$ . The singular spectrum can be clearly  
447 distinguished at  $\tau = 1$ . Therefore, the final parameter pair  $(\tau, L)$  in SSA was set as (1, 9)  
448 for the Wuxi rainfall, and (1, 7) for the other three series. Thus, each rainfall or flow  
449 series can be decomposed into RCs with these identified parameter pair.

### 450 **3.5 Combination of models with SSA**

451 Once an input (rainfall or runoff) time series is decomposed into RCs, the  
452 subsequent task is to filter RCs by finding contributing RCs from all existing RCs to  
453 model output, and then reconstruct a new input series by summing these contributing RCs.

454 There is no practical guide on how to identify a contributing or noncontributing  
455 component to the improvement of accuracy of prediction. Apparently, a single higher-  
456 frequency component may be noncontributing. However, the situation may become  
457 complicated with the combination of components and change of the prediction horizon.  
458 For example, one component viewed as contribution to one-step-ahead prediction may  
459 have a negative impact on two-step-lead prediction. Nevertheless, the combined signal of  
460 several high-frequency RCs may yield a better input/output mapping than a low-  
461 frequency RC. Therefore, an enumeration method is recommended where all input  
462 combinations from rainfall (or runoff) are examined. If the number of RCs is  $L$ , there are  
463  $2^L$  combinations. For instance, there are  $2^9$  combinations for the Wuxi rainfall series in  
464 view of  $L=9$ . It should also be noticed that the enumeration method may be  
465 computationally intensive if  $L$  is a large number, say 20 or 30.

466 Since input variables consist of rainfall and flow, the filtering procedure has to be  
467 conducted separately for each variable. Taking ANN with SSA (hereafter referred to as  
468 ANN-SSA) as an example, two new ANN models need to be established for the purpose  
469 of RCs' filtering, one for rainfall input and the other for runoff input. For the convenience  
470 of identification, the ANN model for rainfall input filtering is denoted by ANN-RF, and  
471 the ANN model for runoff input filtering is referred to as ANN-QF. ANN-RF has the  
472 same model output as that of the original ANN model and its model input is the same as  
473 the rainfall part of the original ANN model inputs. Likewise, the ANN-QF model input is  
474 from the runoff part of the original ANN model inputs, and both of them have the same  
475 model output variable. Depending on trial and error, ANN-RF and ANN-QF can be  
476 identified. For example, ANN-RF was 5-3-1 for Wuxi and 5-4-1 for Chongyang,  
477 respectively, and ANN-QF was 5-4-1 for Wuxi and 4-1-1 for Chongyang, respectively.  
478 Similarly, LR-RF and LR-QF were also developed for the RCs filtering of both rainfall

479 and runoff series in the context of LR. Table 3 presents the RCs filtering results of input  
480 variables of rainfall and runoff for both LR-SSA and ANN-SSA (or MANN-SSA). Two  
481 basic conclusions can be drawn from Table 3 in the context of SSA: one is that ANN-SSA  
482 outperforms LR-SSA with the same model inputs; the model with only runoff input,  
483 either LR-SSA or ANN-SSA, performs better than that with only rainfall input. Therefore,  
484 inclusion of flow in model inputs proves to be imperative in R-R prediction.

#### 485 **4. Results and Discussions**

486 Results of R-R prediction are respectively presented according to the normal mode  
487 and SSA mode. In each mode, three models of LR, ANN, and MANN are compared by  
488 three model performance indices. In the SSA mode, three models are referred to as LR-  
489 SSA, ANN-SSA, and MANN-SSA.

##### 490 **4.1 Predictions in normal mode**

491 As observed from Table 4, all models except for LR for Chongyang have made  
492 one-step-ahead predictions with a high CE over 0.7. This indicates that causal variables of  
493 model output have been accurately selected for this prediction horizon. The performance  
494 of each model deteriorates abruptly with the increase of prediction horizons, which may  
495 indicate the adoption of inappropriate model inputs. Basically, it is intuitive that a poor  
496 prediction on the testing set may result from the lack of similar patterns between the  
497 training set and testing set. Conversely, an excellent prediction probably means that there  
498 are a large number of similar patterns between them. For example, all models perform  
499 better using the Wuxi data than using the Chongyang data since the former has a large  
500 size training data (ten years) which allows models to be appropriately trained. A  
501 conclusion can also be drawn that ANN (or MANN) tends to be superior to LR if the  
502 mapping relation is identified appropriately. The superiority of MANN over ANN seems  
503 to be dependent on the studied data.

504           Figure 8 illustrate representative details of hydrographs and whole scatter plots of  
505 one-step-ahead prediction using three prediction models for Wuxi and Chongyang,  
506 respectively. The scatter plot from the LR model with high spread at low magnitude flows  
507 indicates poor predictions of low flows compared with scatter plots from both ANN and  
508 MANN. ANN and MANN fairly underestimate or overestimate peak flows, but reproduce  
509 low flows appropriately because low flows are more frequent in the data set than large  
510 flows.

511           In order to set up a relative optimal model for runoff prediction, some researchers  
512 carried out runoff predictions depending on ANN (or similar techniques) with two  
513 different inputs: inputs with antecedent runoffs only; and inputs with both antecedent  
514 rainfalls and runoffs. For example, Minns (1998) observed a phase shift error in  
515 prediction outputs when antecedent discharge values were the only inputs used to predict  
516 present discharge. However, models developed using discharge and rainfall inputs were  
517 not observed to exhibit phase shift errors. Sivapragasam et al. (2007) respectively used  
518 GP (genetic programming) and ANN to predict river flows from one- up to four-step  
519 leads with the two types of inputs. Results indicated that the model with rainfall and flow  
520 as inputs, regardless of GP or ANN, made more accurate prediction than that with only  
521 flow input. In this study, we will extend this comparison from the normal mode to the  
522 SSA mode.

523           According to the same method to construct ANN or MANN in the context of  
524 rainfall-runoff transformation as mentioned procedures in Section 3, identified ANNs  
525 with only runoff inputs are 5-3-1 for Wuxi, and 4-8-1 for Chongyang, and identified  
526 MANNs with only runoff inputs are 5-10/10/4-1 for Wuxi, and 4-8/8/5-1 for Chongyang.  
527 In the SSA mode, parameter pair  $(\tau, L)$  is also (1, 7) for each of them.

528           Table 5 presents comparison of runoff predictions using ANN and MANN with  
529 two types of inputs: past flow as the only input variable, and previous rainfall and flow as  
530 input variables. It can be observed that, for the study case of Wuxi, the inclusion of  
531 rainfall in input results in the improvement of model performance irrespective of ANN  
532 and MANN. However, the degree of the improvement mitigates with the increase of  
533 prediction leads. This may indicate that the influence of rainfall on runoff gradually  
534 weakens with the increase of prediction horizons. An opposite result was found by  
535 Sivapragasan et al. (2007) in which the influence of rainfall on runoff (the time resolution  
536 of the data is fortnightly) gradually increased with increasing prediction lead. Employing  
537 the data with an hourly time resolution, Toth and Brath (2007) investigated the  
538 performance of ANN in two types of inputs. They found that ANN with the inclusion of  
539 rainfall in input outperformed ANN with only flow as input at all prediction leads from 1  
540 hour up to 12 hours. Actually, whether or not rainfall is introduced to input heavily relies  
541 on the characteristic of the studied watershed. In general, inclusion of rainfall in input  
542 could be helpful in improving accuracy of predictions if the prediction lead is less than  
543 the average time of concentration. The time of concentration can be roughly identified by  
544 the AMI (or CCF) analysis between available rainfall and flow data, and it approximately  
545 equals the maximum AMI (or CCF). As shown in Figure 5, the time of concentration in  
546 each basin is around one day. If the time resolution of data is hourly-based, the time of  
547 concentration can be approximated to hours but days. Therefore, the inclusion of rainfall  
548 in input has led to a noticeable improvement of accuracy of one-day-ahead prediction. In  
549 this regard, a more detailed analysis will be addressed in the section of discussions.

550           The hydrograph of one-step-ahead prediction is presented in Figure 9. The ANN  
551 model with only flow input makes the lagged predictions whereas the ANN model with  
552 rainfall and flow as inputs eliminates the lag effect. However, with the increase of

553 prediction leads, each of two types of ANN yields a prediction lag effect as shown in  
554 Figure 10, which indicates the effect of rainfall on model output being markedly mitigated.

#### 555 **4.2 Predictions in SSA mode**

556 Table 6 presents the results of R-R predictions for Wuxi and Chongyang using  
557 three prediction models coupled with SSA. Compared with the results of Table 4, the SSA  
558 technique brings about a significant improvement of model performance at all three  
559 prediction horizons. Models of ANN and MANN outperform the LR model, but the  
560 MANN model exhibits no superiority over the ANN model.

561 The representative details of hydrograph and whole scatter plots of one-step-ahead  
562 prediction for Wuxi and Chongyang are shown in Figure 11. These results show that three  
563 models with SSA are able to make good predictions because the predicted hydrograph  
564 perfectly reproduces the actual hydrograph and the scatter plots are close to the exact line  
565 with rather a low spread. It can be observed from the hydrograph that the LR-SSA model  
566 produces some negative predictions for the low flows and ANN-SSA and MANN-SSA  
567 occasionally make negative predictions at the low-flow points. The peak values are still  
568 overestimated or underestimated although each model with SSA exhibits excellent overall  
569 performances.

570 Table 7 presents comparison of two types of model inputs feeding ANN-SSA and  
571 MANN-SSA. ANN-SSA (or MANN-SSA) fed by rainfall and flow performs better than  
572 the corresponding model fed by only flow at all prediction leads. It is observed that the  
573 advantage of models with rainfall and flow inputs over those with flow input only  
574 becomes more obvious with increasing prediction leads, which indicates that SSA  
575 improves the dependence relation more significantly between rainfall and flow than that  
576 between flows itself. The model output may therefore depend more on rainfall inputs  
577 instead of flow itself when the prediction lead is larger than one day.



578 Figure 12 illustrates one-step-ahead prediction hydrographs for Wuxi and  
579 Chongyang using ANN-SSA in two types of inputs. ANN-SSA with rainfall and flow  
580 inputs better captures the peak flows, and reproduces the actual hydrograph more  
581 smoothly whereas the hydrograph from ANN-SSA with flow input only is serrated at  
582 some locations. It is found that there is no time shift between the predicted hydrograph  
583 and the actual one. Figure 13 demonstrates the results of lag effect analysis at all three  
584 prediction horizons by depicting CCF between observation and prediction. SSA  
585 eradicates the prediction lag effect in the ANN model regardless of model input types.  
586 Moreover, it can be observed that the CCF curve in ANN-SSA with rainfall and flow  
587 inputs is more symmetrical than that in ANN-SSA with only flow input, which reveals  
588 that predictions in the former is in better agreement with the observations in time.

### 589 **4.3 Discussions**

590 The following discussions focus on two aspects: investigating the difference  
591 between two types of model inputs for runoff prediction, and investigating the effect of  
592 SSA on the R-R ANN model inputs.

#### 593 **a) Analysis of model inputs**

594 As shown in Table 5, ANN with rainfall and flow inputs performs better than that  
595 with flow input only at all prediction leads, but the improvement of model performance  
596 decreases abruptly at a two-step lead. A direct explanation for that phenomenon is that the  
597 impact of rainfall on runoff weakens suddenly at two-step-ahead prediction, which can be  
598 examined by AMI and CCF between model inputs and output.

599 Figure 14(a) presents AMI between each input and output of ANN in two model  
600 input scenarios for the Wuxi study case. The number of model inputs in the abscissa axis  
601 consists of 5 previous flow data and 4 previous rainfall data. The former 5 inputs stand for  
602 5 past flows and the latter 5 inputs denote 5 past rainfall observations. In contrast, all 10

603 model inputs (actually 5) in the flow input scenario are the past 10 flow observations.  
604 First of all, it is clearly shown from all three sub-plots that AMI associated with each  
605 model input decreases significantly with an increase in the prediction lead, which may  
606 indicate decrease of the overall dependence relation between model inputs and output.  
607 Therefore, it provides a potential explanation for the trend in Table 6 that the accuracy of  
608 the prediction decreases with the increase of prediction horizons. Secondly, the nearest  
609 rainfall observation (the sixth model input in each plot) to the prediction horizon has the  
610 maximum AMI, so inclusion of such input improves the prediction. Some of the other  
611 rainfall inputs also have reasonably larger AMI compared to that of flow inputs, and they  
612 also contribute to the improvement of model performance.

613 Figure 14(b) shows AMI of each input and output of ANN with two types of  
614 inputs for the Chongyang study case. Regarding ANN in rainfall and flow inputs, the first  
615 4 model inputs in the abscissa axis are from the past flows and the latter 5 inputs represent  
616 the 5 last rainfall observations. As far as ANN with flow input only is concerned, the first  
617 4 model inputs in the abscissa axis are the actual inputs. It can be observed that, AMI of  
618 each model input and output between two-step-ahead and three-step-ahead predictions is  
619 similar and very small regardless of the input scenario. Moreover, the holistic AMI from  
620 rainfall inputs does not dominate over the overall AMI from flow inputs. Therefore,  
621 inclusion of such rainfall inputs may only make the training process computation  
622 intensive without any tangible improvement in prediction accuracy. As a consequence,  
623 the model performance of ANN with two types of inputs is similarly poor for both two-  
624 and three-step-ahead predictions (depicted as Table 5). On the contrary, for one-step-  
625 ahead prediction, the nearest two rainfall inputs have large AMIs which are only smaller  
626 than the AMI of the immediate past flow input. As expected, their inclusion in model

627 inputs improves the overall mapping between inputs and output of ANN, making one-  
628 step-ahead prediction with good accuracy.

629         The static multi-step prediction method is adopted in this study. The poor  
630 prediction at two- or three-step-ahead horizon using ANN with rainfall and flow as inputs  
631 may be improved by adopting a dynamic ANN model instead of the current static ANN  
632 model. In the dynamic ANN model, the predicted flow and rainfall in the last step are  
633 used as the nearest flow and rainfall inputs in the present prediction step, and then a  
634 multi-step prediction becomes a repeated one-step prediction. However, de Vos and  
635 Rientjes (2005) mentioned that for both the daily and hourly data the two multi-step  
636 prediction methods performed nearly similar up to a lead time of respectively 4 days and  
637 12 hours. Similarly, the results from Yu et al. (2006) for hourly data also showed that two  
638 methods could yield similar predictions.

#### 639 **b) Investigation of the SSA effect on model inputs**

640         Herein, the effect of SSA on inputs of an ANN R-R model is investigated by AMI  
641 between each input and output of model. Results of prediction from the ANN R-R model  
642 with the normal mode (shown in Tables 4 or 5) show that the flows at one-step lead are  
643 predicted appropriately whereas poor predictions are obtained at two- or three-step lead.  
644 Correspondingly, it can be observed from Figure 15(a) that AMI associated with each  
645 model input for one-step prediction is far larger than the counterparts for two- or three-  
646 step predictions. Figure 15(b) shows that SSA improved AMI of each input at all three  
647 prediction horizons. The AMI curve of filtered inputs between one- and two-step  
648 predictions is very similar, which may indicate similar model performance (shown in  
649 Tables 6 or 7 where the model performance at the two prediction leads is also quite  
650 similar). Therefore, the AMI analysis proves to be able to reveal the suitability of a  
651 prediction model to some extent. Figure 15(b) also reveals that AMI at one-step

652 prediction is far larger than that at two- and three-step leads. So the prediction accuracy at  
653 the former is markedly superior to that in the latter (shown in Tables 4 or 5). In the SSA  
654 mode, AMI of each input is considerably improved at all prediction horizons, which  
655 renders the ANN-SSA R-R model good predictions (shown in Tables 6 or 7) in  
656 comparison to that in the normal mode.

## 657 **5. Conclusions**

658 This study has predicted daily rainfall-runoff transformation from two different  
659 watersheds, namely Wuxi and Chongyang, through three models (viz. LR, ANN and  
660 MANN) in conjunction with SSA. Rainfall and runoff are firstly identified as appropriate  
661 input variables, and then model inputs are selected by LCA after comparison with the  
662 other four methods of determining model inputs. The model performance seems to be  
663 sensitive to the studied case in the normal mode. For Wuxi, the MANN R-R model  
664 (namely, rainfall and runoff as inputs) outperforms the ANN R-R model and the ANN R-  
665 R model performs better than the LR R-R model at all three prediction horizons. For  
666 Chongyang, the ANN R-R model performs the best among three models at one-step lead.  
667 However, they are similar at the other two prediction horizons. In the SSA mode, the  
668 performance of each model is significantly improved. Both ANN-SSA and MANN-SSA  
669 have similar performance and achieve better results than LR-SSA.

670 The ANN R-R model is also compared with the ANN model with only runoff  
671 input. The ANN R-R model outperforms the ANN model with only flow input in both the  
672 normal mode and SSA mode. The degree of superiority tends to mitigate with the increase  
673 of prediction leads in the normal mode. However, situation becomes reverse in the SSA  
674 mode where the advantage of the ANN R-R model seems to be more remarkable with the  
675 increase of prediction leads. It is recommended from the present study that the ANN R-R  
676 model coupled with SSA is more promising.

677

678 **References:**

679 Abebe, A.J., and Price, R.K. (2003), Managing uncertainty in hydrological models using  
680 complementary models. *Hydrological Sciences Journal-Journal des Sciences  
681 Hydrologiques*, 48 (5), 679-692.

682 Abrahart, R.J., See, L.M., and Kneale, P.E. (1999), Using pruning algorithms and genetic  
683 algorithms to optimise network architectures and forecasting inputs in a neural network  
684 rainfall-runoff model. *Journal of Hydroinformatics*, 1, 103-114.

685 Abrahart, R.J., See, L.M., and Kneale, P.E. (2001), Applying saliency analysis to neural  
686 network rainfall-runoff modelling. *Computers and Geosciences*, 27, 921-928.

687 Anctil, F., Perrin, C., and Andréassian, V. (2004), Impact of the length of observed  
688 records on the performance of ANN and of conceptual parsimonious rainfall-runoff  
689 forecasting models. *Environmental Modeling and Software*, 19, 357-368.

690 ASCE. (2000), Artificial neural networks in hydrology 2: Hydrology applications. *Journal  
691 of Hydrologic Engineering*, 5(2), 124-137.

692 Baratta et al., Baratta, D., Cicioni, G., Masulli, F. and Studer, L. (2003), Application of an  
693 ensemble technique based on singular spectrum analysis to daily rainfall forecasting.  
694 *Neural Networks*, 16, 375-387.

695 Bezdek, J.C. (1981), *Pattern Recognition with Fuzzy Objective Function Algorithms*.  
696 Plenum Press, New York.

697 Birikundavyi, S., Labib, R., Trung, H.T., and Rousselle, J. (2002), Performance of neural  
698 networks in daily streamflow forecasting. *Journal of Hydrologic Engineering*, 7(5), 392-  
699 398.

700 Campolo, M., Andreussi, P., and Soldati, A. (1999), River flood forecasting with a neural  
701 network model, *Water Resources Research*, 35 (4), 1191-1197.

- 702 Corzo, G., and Solomatine, D. (2007), Baseflow separation techniques for modular  
703 artificial neural network modelling in flow forecasting. *Hydrological Sciences–Journal–*  
704 *des Sciences Hydrologiques*, 52(3), 491-507.
- 705 Coulibaly, P., Anctil, F., and Bobée, B. (2000), Daily reservoir inflow forecasting using  
706 artificial neural networks with stopped training approach *Journal of Hydrology*, 230, 244-  
707 257.
- 708 Coulibaly, P., Anctil, F., and Bobée, B. (2001), Multivariate reservoir inflow forecasting  
709 using temporal neural networks. *Journal of Hydrologic Engineering*, 6 (5), 367-376.
- 710 Dawson, C.W., and Wilby, R.L. (2001), Hydrological Modeling Using Artificial Neural  
711 Networks. *Progress in Physical Geography*, 25(1), 80-108.
- 712 de Vos, N.J. and Rientjes, T.H.M. (2005), Constraints of artificial neural networks for  
713 rainfall -runoff modeling: trade-offs in hydrological state representation and model  
714 evaluation. *Hydrology and Earth System Sciences*, 9, 111-126.
- 715 Dibike, Y. B. and Solomatine, D. P. (2001), River flow forecasting using artificial neural  
716 networks, *Physics and Chemistry of the Earth (B)*, 26 (1), 1-7, 2001.
- 717 Draper, N. R. and Smith, H. (1998), *Applied regression analysis*, 3rd ed. New York:  
718 Wiley.
- 719 Elsner, J., and Tsonis, A. (1996), *Singular Spectrum Analysis. A New Tool in Time*  
720 *Series Analysis*. New York: Plenum Press.
- 721 Fraser, A.M. and Swinney, H.L. (1986), Independent coordinates for strange attractors  
722 from mutual information, *Physical Review A*, 33(2), 1134-1140.
- 723 Giustolisi, O., and Savic, D. A. (2006), A symbolic data-driven technique based on  
724 evolutionary polynomial regression, *Journal of Hydroinformatics*, 8(3), 207-222.
- 725 Golyandina, N. Nekrutkin, V., and Zhigljavsky, A. (2001), *Analysis of Time Series*  
726 *Structure: SSA and Related Techniques*, Chapman & Hall/CRC.

- 727 Hsu, K.L., Gupta, H.V., and Sorooshian, S. (1995), Artificial neural network modeling of  
728 the rainfall–runoff process. *Water Resources Research*, 31(10), 2517-2530.
- 729 Hu, T.S., Wu, F.Y., and Zhang, X. (2007), Rainfall-runoff modeling using principal  
730 component analysis and neural network. *Nordic Hydrology*, 38(3), 235-248.
- 731 Jain, A., and Srinivasulu, S. (2004), Development of effective and efficient rainfall-runoff  
732 models using integration of deterministic, real-coded genetic algorithms and artificial  
733 neural network techniques, *Water Resource Research*, 40, W04302.
- 734 Jain, A., and Srinivasulu, S. (2006), Integrated approach to model decomposed flow  
735 hydrograph using artificial neural network and conceptual techniques. *Journal of*  
736 *Hydrology*, 317, 291-306.
- 737 Kitanidis, P. K. and Bras, R. L. (1980), Real-time forecasting with a conceptual  
738 hydrologic model, 2, applications and results, *Water Resources Research*, 16 (6), 1034–  
739 1044.
- 740 Kumar, A.R.S., Sudheer, K.P., Jain, S.K., and Agarwal, P.K. (2005), Rainfall-runoff  
741 modelling using artificial neural networks: comparison of network types. *Hydrological*  
742 *Processes*, 19 (6), 1277-1291.
- 743 Legates, D. R., and McCabe, Jr, G. J. (1999), Evaluating the use of goodness-of-fit  
744 measures in hydrologic and hydroclimatic model validation, *Water Resources. Research*,  
745 35(1), 233- 241.
- 746 Liong, S. Y., Gautam, T. R., Khu, S. T., Babovic, V., and Muttill, N. (2002), Genetic  
747 programming: A new paradigm in rainfall-runoff modeling. *Journal of American Water*  
748 *Resources Association*, 38(3), 705-718.
- 749 Lisi, F., Nicolis, and Sandri, M. (1995), Combining singular-spectrum analysis and neural  
750 networks for time series forecasting. *Neural Processing Letters*, 2(4), 6-10.
- 751 Maier H.R., and Dandy G.C. (2000), Neural networks for the prediction and forecasting

- 752 of water resources variables: a review of modeling issues and applications. *Environmental*  
753 *Modeling and Software*, 15, 101-23.
- 754 Marques, C.A.F., Ferreira, J., Rocha, A., Castanheira, J., Gonçalves, P., Vaz, N., and Dias,  
755 J.M. (2006), Singular spectral analysis and forecasting of hydrological time series.  
756 *Physics and Chemistry of the Earth*, 31, 1172-1179.
- 757 May, R.J., Maier, H.R., Dandy, G.C., and Fernando, T.M.K. (2008), Non-linear variable  
758 selection for artificial neural networks using partial mutual information. *Environmental*  
759 *Modeling & Software*, 23, 1312-1328.
- 760 McCuen, R. H. (2005), *Hydrologic analysis and design* (3rd ed.), Upper Saddle River, NJ:  
761 Pearson/Prentice Hall.
- 762 Minns, A. W. (1998), *Artificial Neural Networks as Subsymbolic Process Descriptors*.  
763 Balkema, Rotterdam, The Netherlands.
- 764 Mulvany, T. J. (1850), On the use of self-registering rain and flood gauges. *Proc. Inst. Civ.*  
765 *Eng.*, 4(2), 1–8.
- 766 Nash, J. E. and Sutcliffe, J. V. (1970), River flow forecasting through conceptual models  
767 part I — A discussion of principles. *Journal of Hydrology*, 10 (3), 282-290.
- 768 Sajikumar, N., and Thandaveswara, B.S. (1999), A non-linear rainfall-runoff model using  
769 artificial neural networks. *Journal of Hydrology*, 216, 32-55.
- 770 Shamseldin, A.Y. (1997), Application of a neural network technique to rainfall–runoff  
771 modelling. *Journal of Hydrology* 199, 272-294.
- 772 Sivapragasam, C., Liong, S.Y. and Pasha, M.F.K. (2001), Rainfall and runoff forecasting  
773 with SSA-SVM approach. *Journal of Hydroinformatics*, 3(7), 141-152.
- 774 Sivapragasam, C., Vincent and, P., and Vasudevan, G. (2007), Genetic programming  
775 model for forecast of short and noisy Data. *Hydrological Processes*, 21, 266-272.
- 776 Solomatine, D., and Dulal, K. (2003), Model trees as an alternative to neural networks in



- 777 rainfall–runoff modelling. *Hydrological Sciences Journal*, 48(3), 399-411.
- 778 Solomatine, D.P., and Shrestha, D.L. (2009), A novel method to estimate model  
779 uncertainty using machine learning techniques. *Water Resources Research*, 45, W00B11,  
780 doi:10.1029/2008WR006839.
- 781 Solomatine, D. P. and Xue, Y. I. (2004), M5 model trees and neural networks: application  
782 to flood forecasting in the upper reach of the Huai River in China. *Journal of*  
783 *Hydrological Engineering*, 9(6), 491-501.
- 784 Sudheer, K. P., Gosain, A. K., and Ramasastri, K. S. (2002), A data-driven algorithm for  
785 constructing artificial neural network rainfall-runoff models. *Hydrological Processes*, 16,  
786 1325-1330.
- 787 Tokar, A.S., and Johnson, P.A. (1999), Rainfall–runoff modeling using artificial neural  
788 networks. *Journal of Hydrologic Engineering*, 4(3), 232-239.
- 789 Toth, E., and Brath, A. (2007), Multistep ahead streamflow forecasting: Role of  
790 calibration data in conceptual and neural network modeling. *Water Resources Research*,  
791 43(11), art. no. W11405.
- 792 Wang, W., Van Gelder, P.H.A.J.M., Vrijling, J.K. and Ma, J. (2006), Forecasting Daily  
793 Streamflow Using Hybrid ANN Models. *Journal of Hydrology*, 324, 383-399.
- 794 Wilby, R.L., Abrahart, R.J., and Dawson, C. W. (2003), Detection of conceptual model  
795 rainfall-runoff processes inside an artificial neural network. *Hydrological Sciences*  
796 *Journal*, 48(2), 163-181.
- 797 Wu, C.L., Chau, K.W., Fan, C. (2010), Prediction of rainfall time series using modular  
798 artificial neural networks coupled with data-preprocessing techniques. *Journal of*  
799 *Hydrology*, 389 (1-2), 146-167.
- 800 Xu, Z.X., and Li, J.Y. (2002), Short-term inflow forecasting using an artificial neural  
801 network model. *Hydrological Processes*, 16(12), 2423-2439.

802 Yu, P.S., Chen, S.T., and Chang I.F. (2006), Support vector regression for real-time flood  
803 stage forecasting. *Journal of hydrology*, 328,704-716.

804 Zealand, C. M., Burn, D. H., and Simonovic, S. P. (1999), Short term stream flow  
805 forecasting using artificial neural networks. *Journal of Hydrology*, 214, 32-48.

806 Zhang, B., and Govindaraju, R. S. (2000), Prediction of watershed runoff using Bayesian  
807 concepts and modular neural networks. *Water Resources Research*, 36(3), 753-762.

808

809 **Figure Captions**

810

811 Figure 1 Daily rainfall-runoff time series: (a) Wuxi and (b) Chongyang

812 Figure 2. Flow chart of MANN

813 Figure 3. Implementation framework of forecasting models

814 Figure 4. Plots of ACF and PACF of the runoff series with the 95% confidence bounds

815 (the dashed lines), (a) and (c) for Wuxi, and (b) and (d) for Chongyang

816 Figure 5. CCFs between rainfall and flow series with the 95% confidence bounds (the

817 dashed lines): (a) for Wuxi, and (b) for Chongyang.

818 Figure 6. Singular Spectrum as a function of lag using varied window lengths  $L$  from 3 to

819 10: (a) and (c) for Wuxi, and (b) and (d) for Chongyang.

820 Figure 7. Sensitivity analysis of singular Spectrum on varied  $\tau$  : (a) and (c) for Wuxi and

821 (b) and (d) for Chongyang.

822 Figure 8. Hydrographs (representative details) and scatter plots of one-step-ahead

823 prediction for (a) Wuxi and (b) Chongyang.

824 Figure 9. Hydrographs for one-step-ahead prediction using ANN with two types of inputs:

825 (a) Wuxi, and (b) Chongyang.

826 Figure 10. Lag analysis of observation and forecasts of ANN with two types of inputs: (a)

827 and (c) for Wuxi, and (b) and (d) for Chongyang.

828 Figure 11. Hydrographs (representative details) and scatter plots of one-step-ahead

829 prediction in SSA mode for (a) Wuxi and (b) Chongyang.

830 Figure 12. Hydrographs for one-step-ahead prediction using ANN-SSA with two types of

831 inputs: (a) Wuxi, and (b) Chongyang.

832 Figure 13. Lag analysis of observation and forecasts of ANN-SSA with two types of

833 inputs: (a) and (c) for Wuxi, and (b) and (d) for Chongyang.

834 Figure 14. AMIs between model inputs and output for ANN with two types of inputs  
835 using the data of (a) Wuxi and (b) Chongyang.

836 Figure 15. AMIs between model inputs and output for ANN and ANN-SSA in the context  
837 of R-R forecasting using the data of (a) Wuxi and (b) Chongyang.

838

839 **Table Captions**

840 Table 1. Statistical information on rainfall and streamflow data

841 Table 2. Comparison of methods to determine mode inputs using ANN

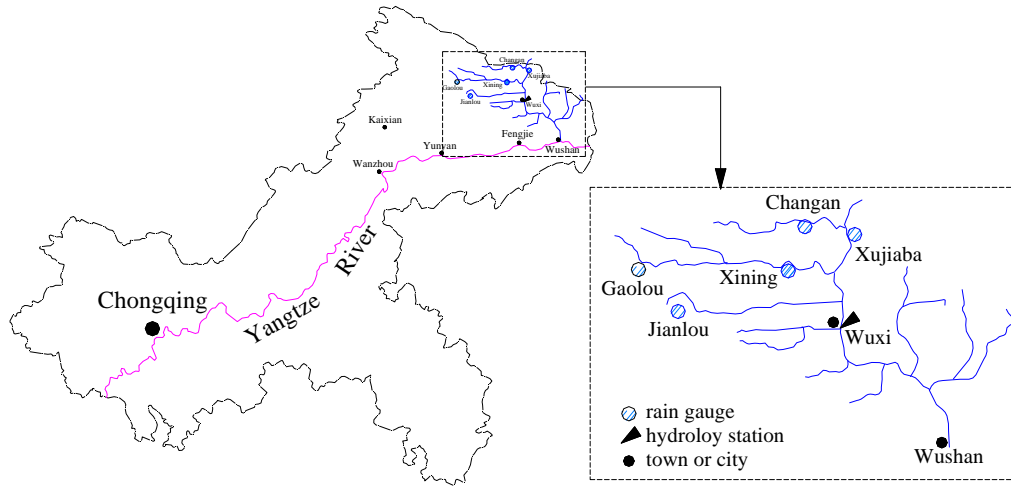
842 Table 3. Optimal  $p$  RCs of rainfall and runoff input variables at various forecast horizons

843 Table 4. R-R Model performances at three forecasting horizons in the normal mode

844 Table 5. Performances of ANN and MANN in two types of input variables

845 Table 6. Performances of R-R models in the SSA mode

846 Table 7. Performances of ANN-SSA and MANN-SSA using two types of input variables

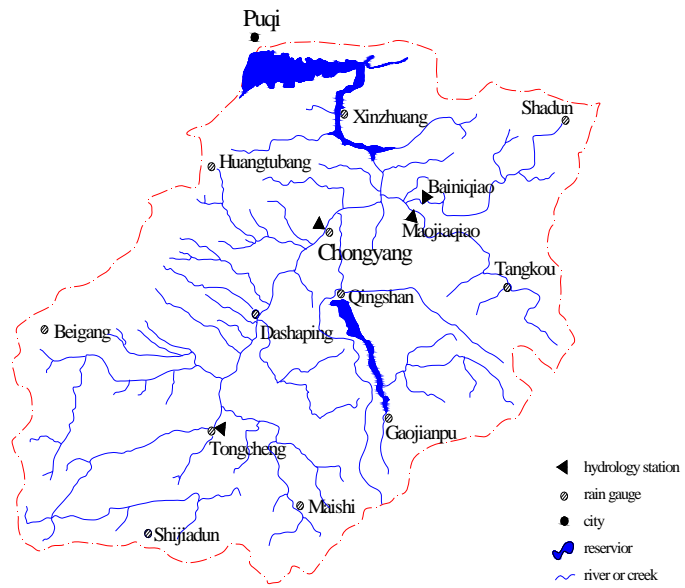


1  
2  
3

Figure1.

4

5



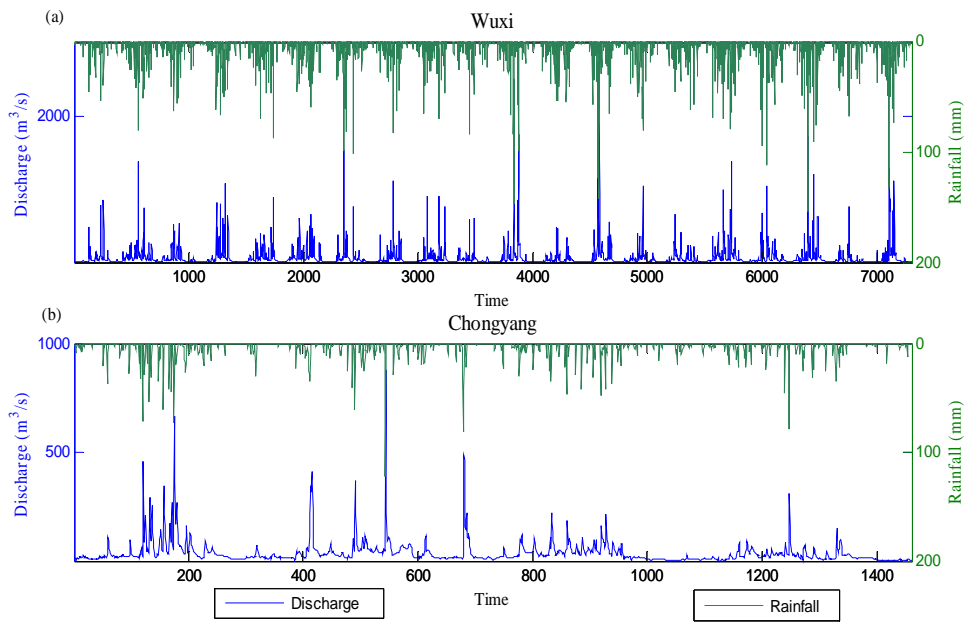
6

7

8

Figure 2

9



10  
11  
12

Figure 3

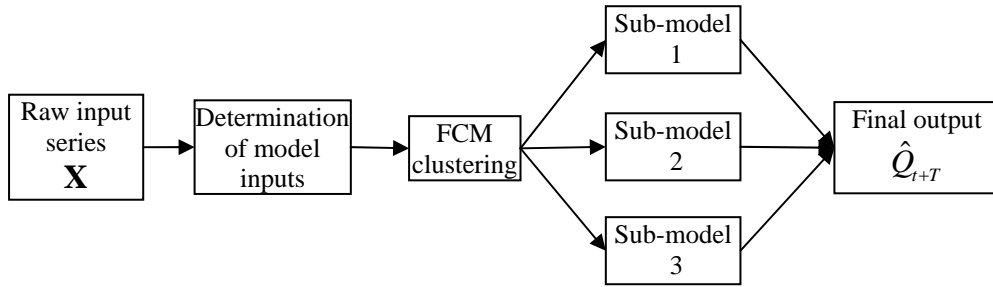


13

14

15

16



17

18

19

20

Figure 4.

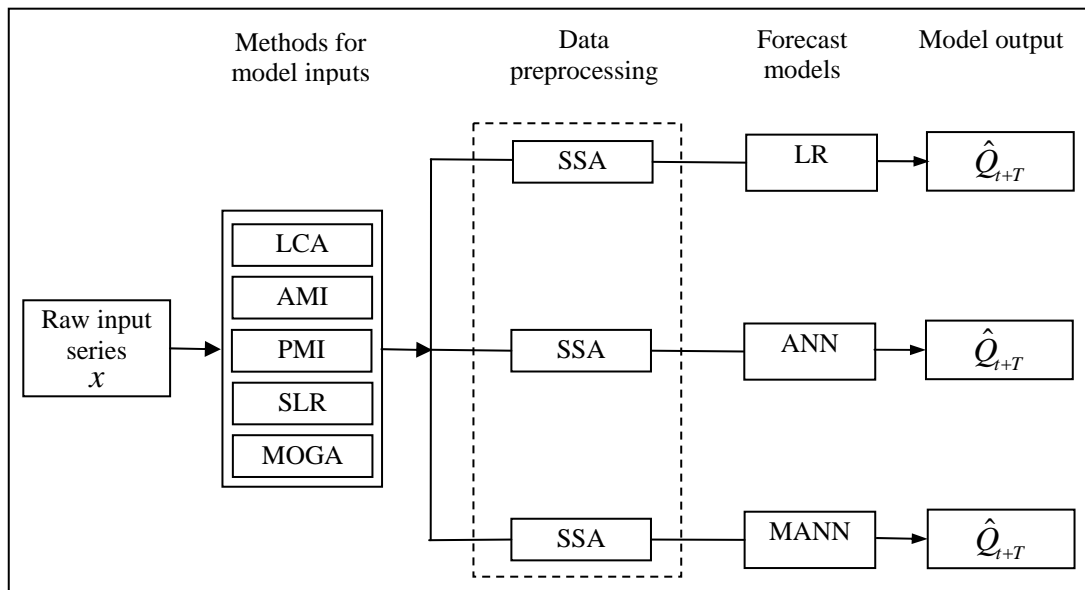
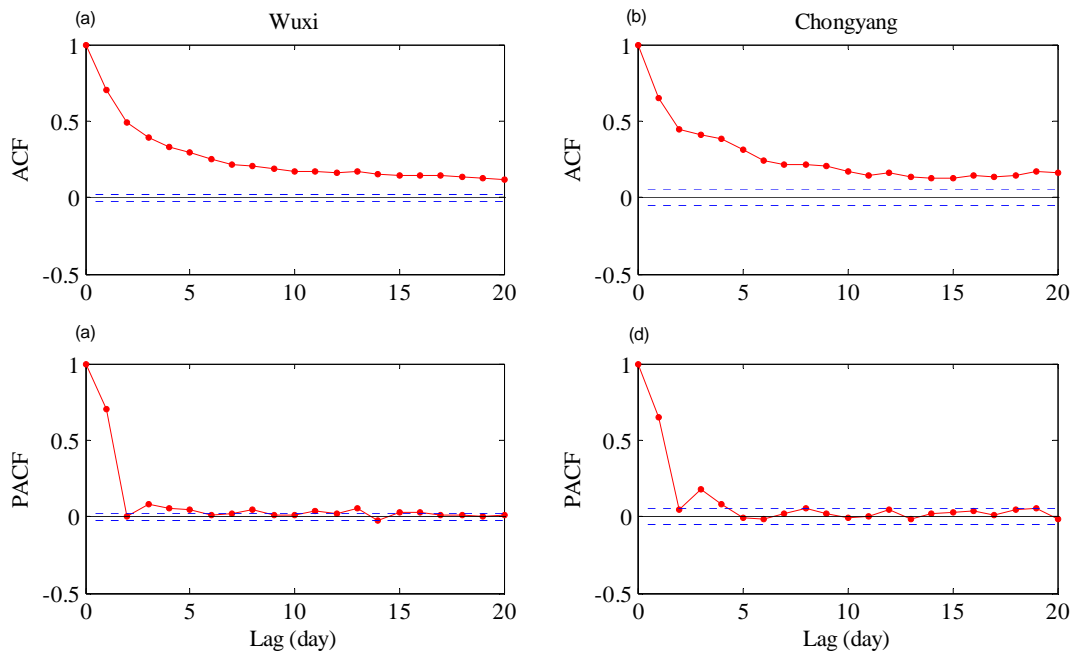


Figure 5.

25

26



27

28

29

Figure 6.

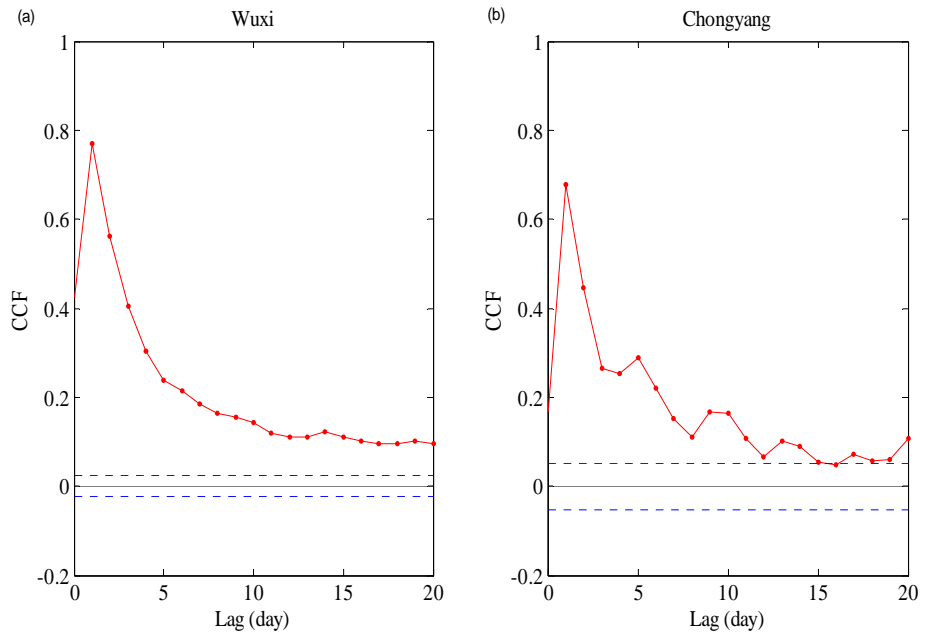
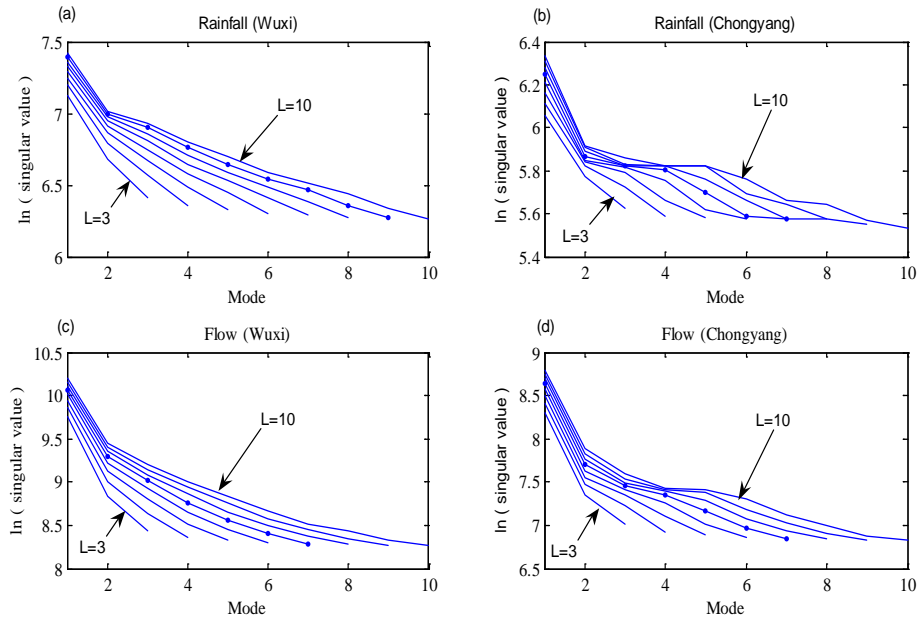


Figure 7.

30  
31  
32

33

34



35

36

37

38

Figure 8.

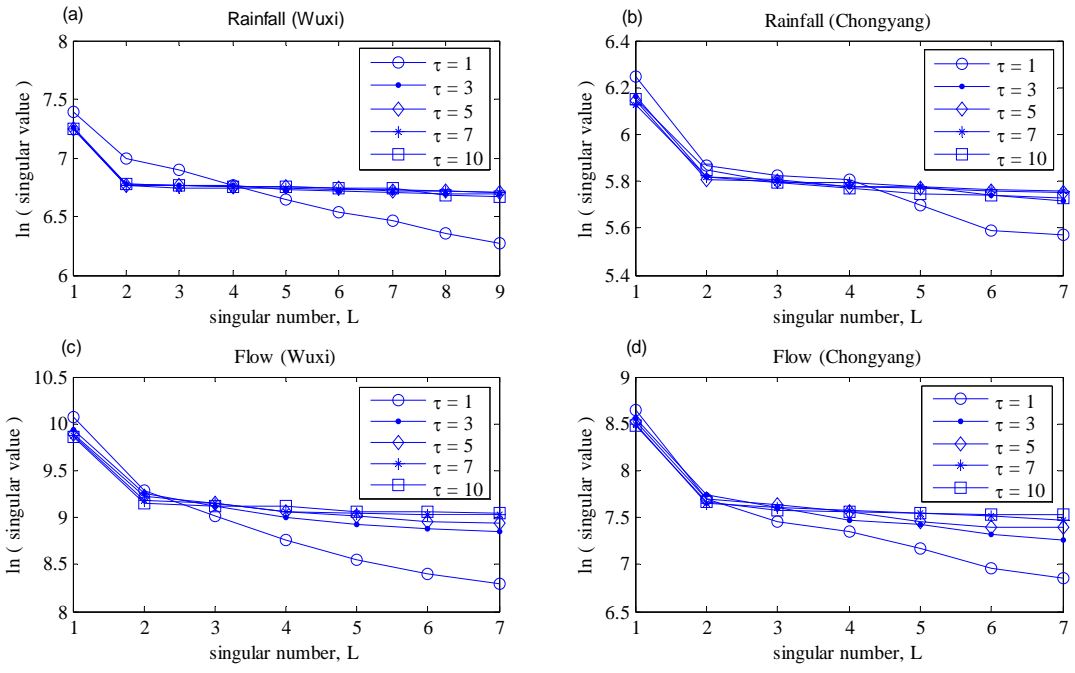
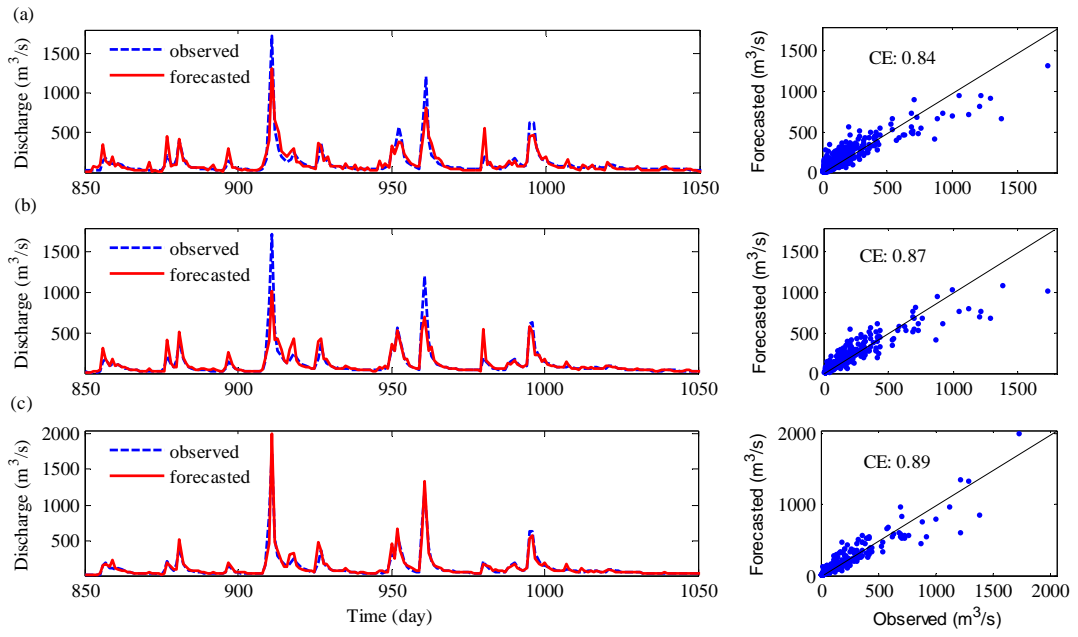


Figure 9

39  
40  
41

42

43



44

45

46

Figure 10.

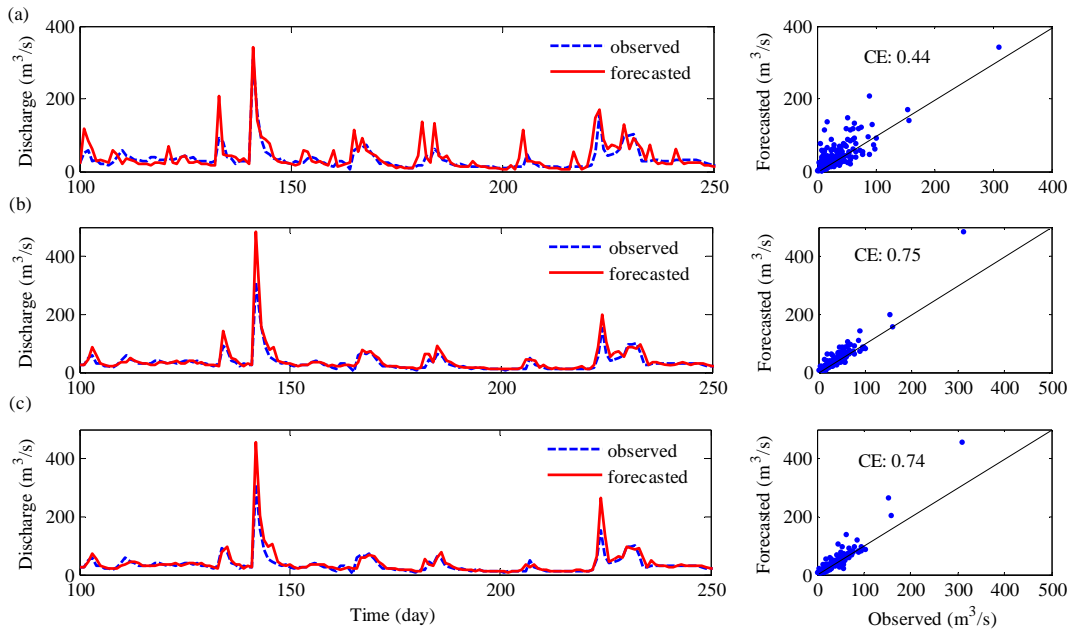
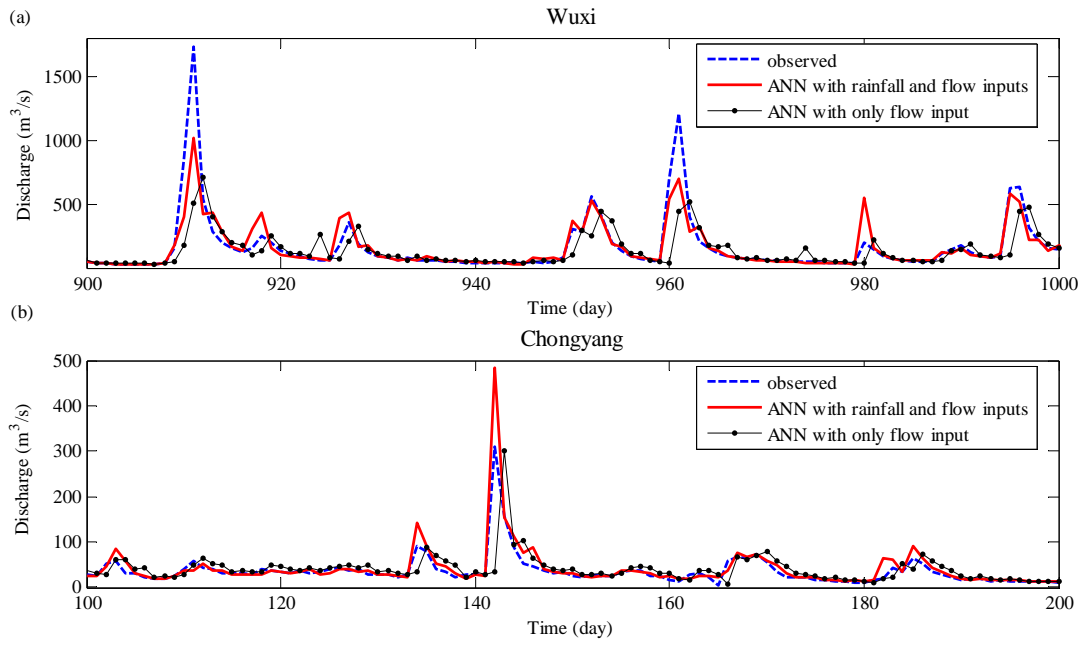


Figure 11.



51

52



53

54

Figure 12.

55

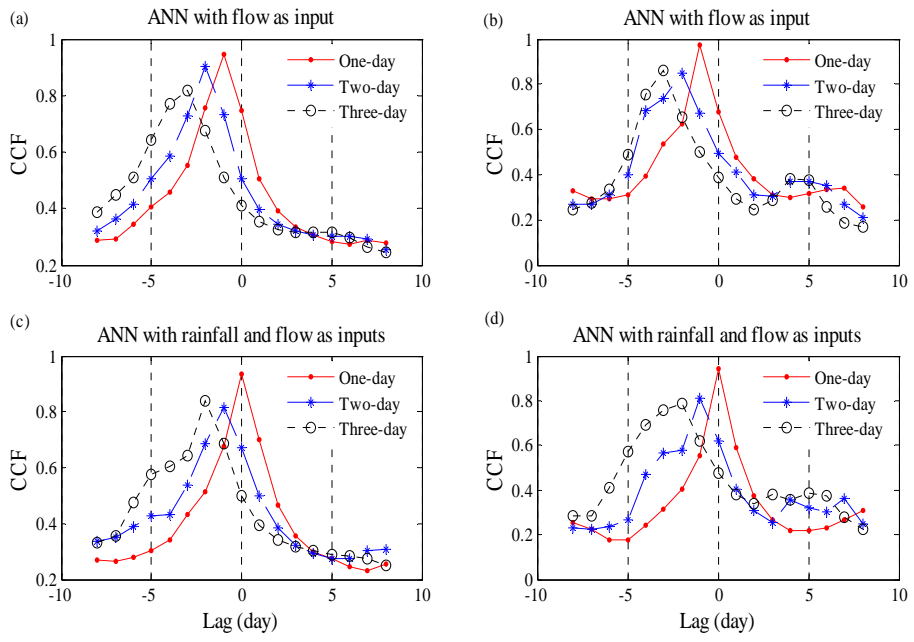
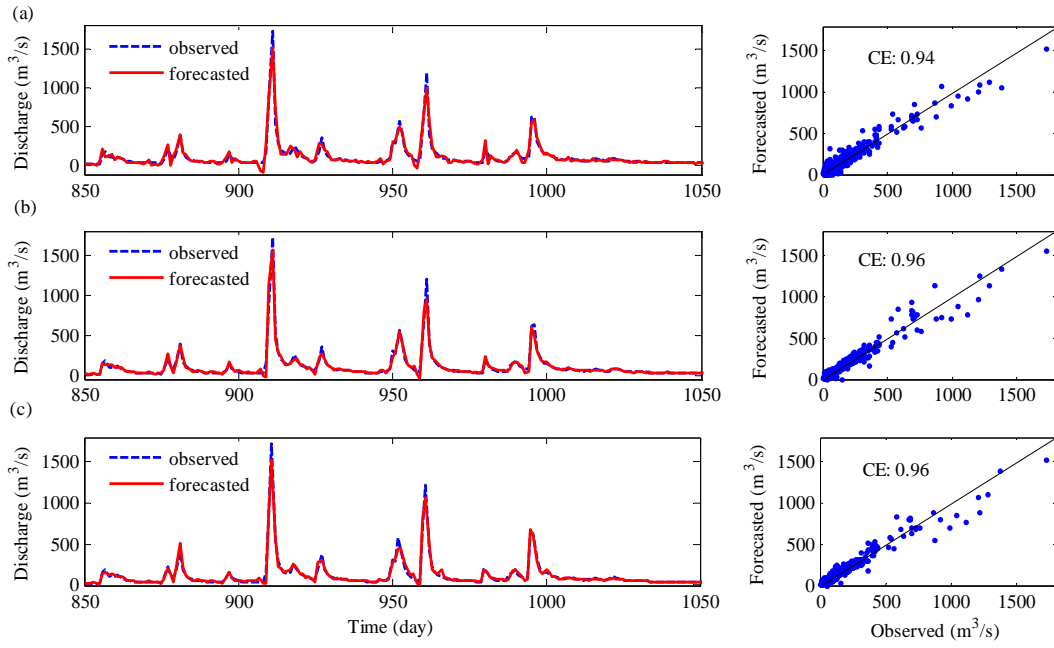


Figure 13.

60

61



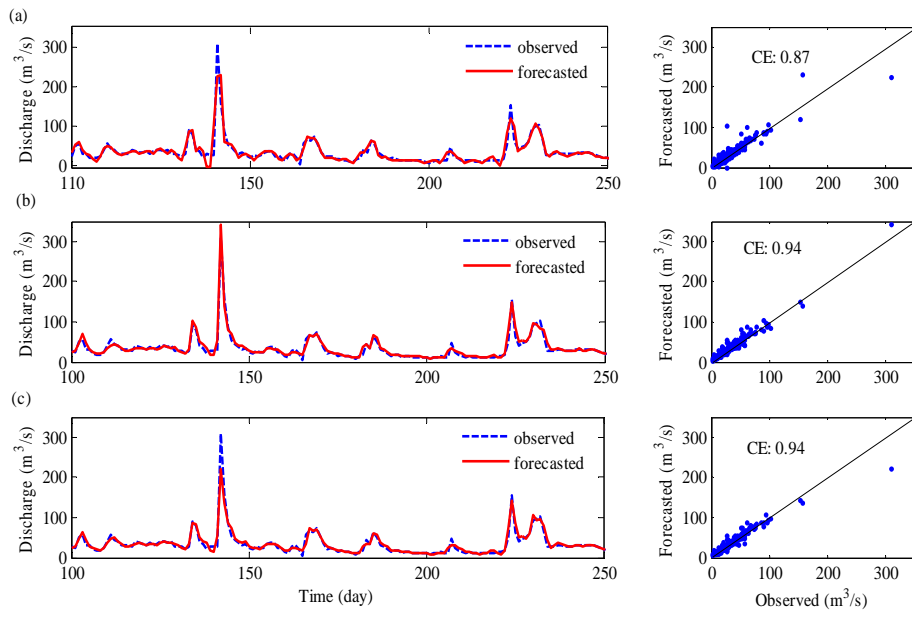
62

63

64

Figure 14.

65



66

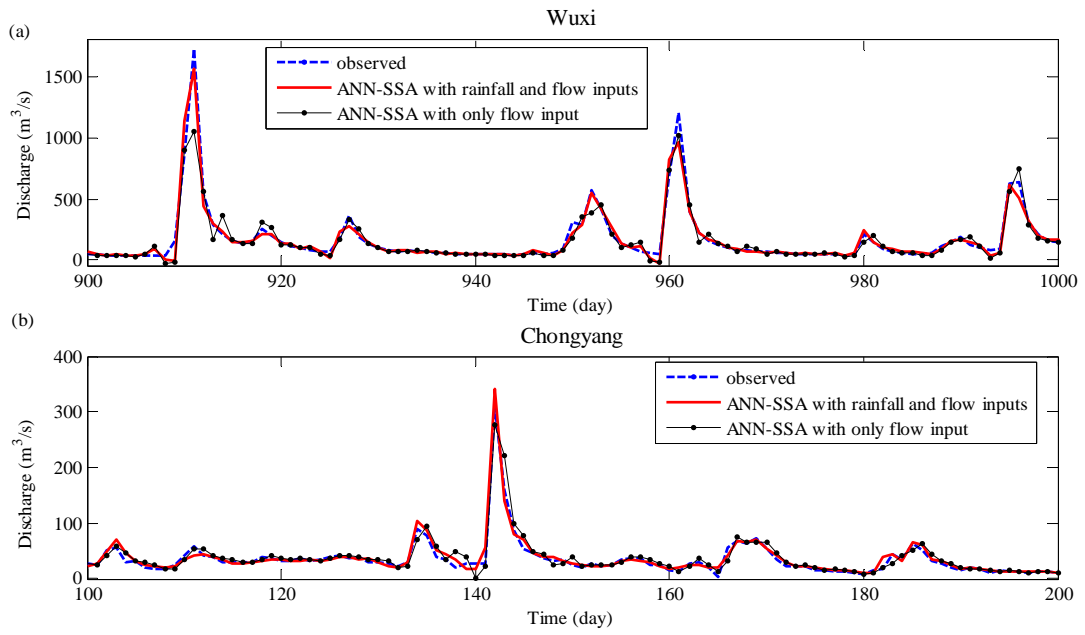
67

68

Figure 15.

69

70

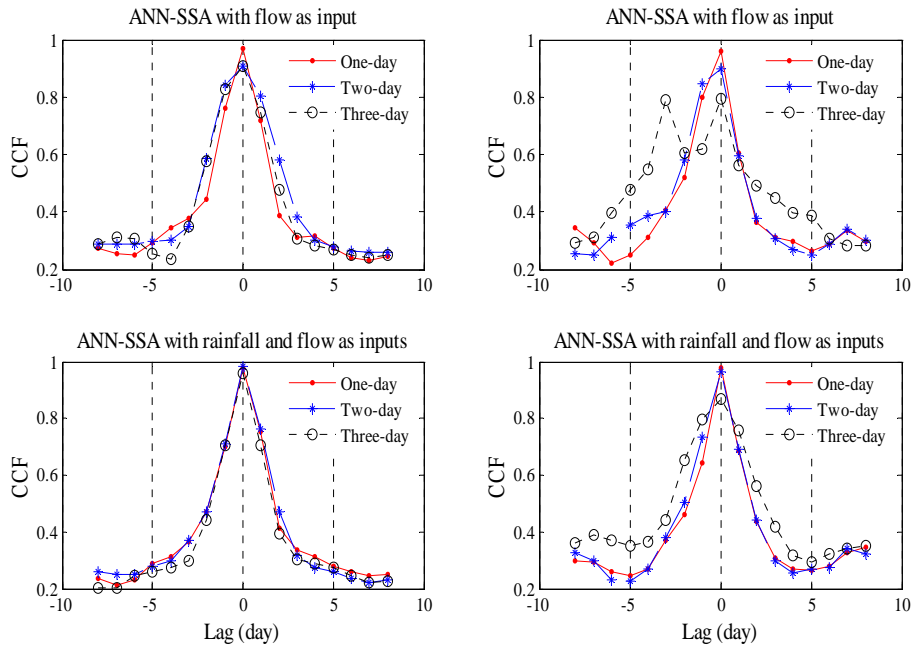


71

72

Figure 16.

73



74

75

76

Figure 17.

77

78

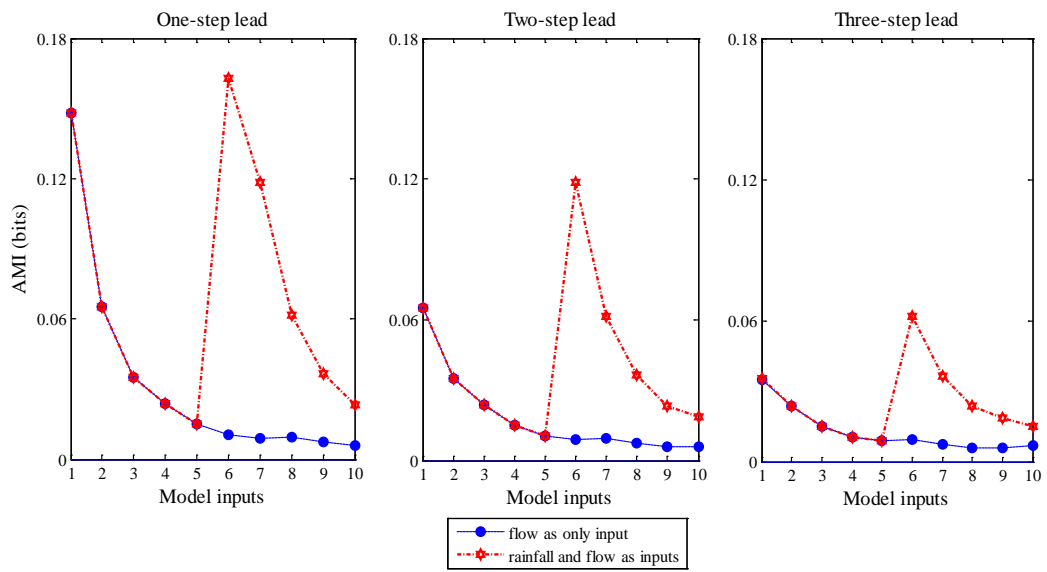


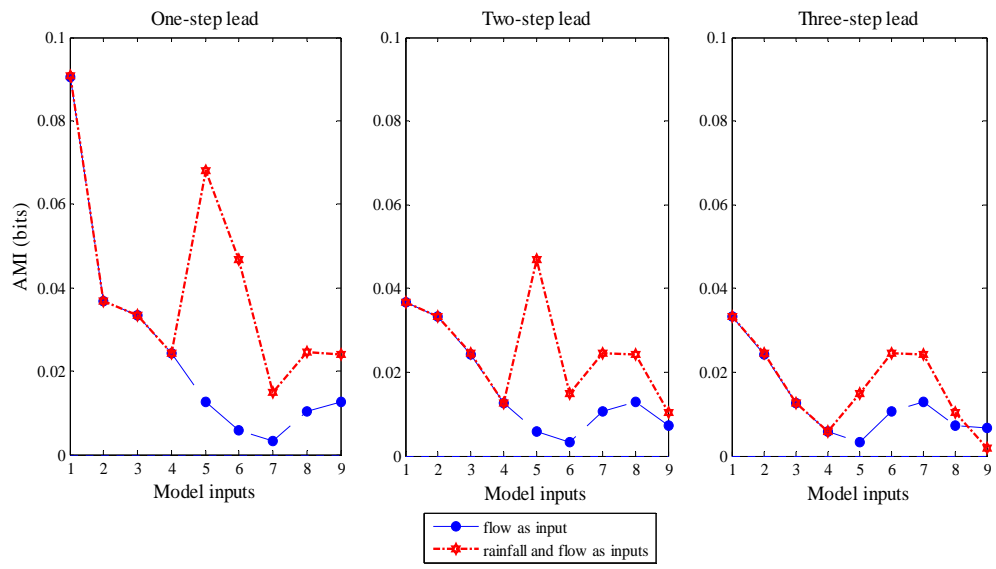
Figure 18.

79

80

81

82



83

84

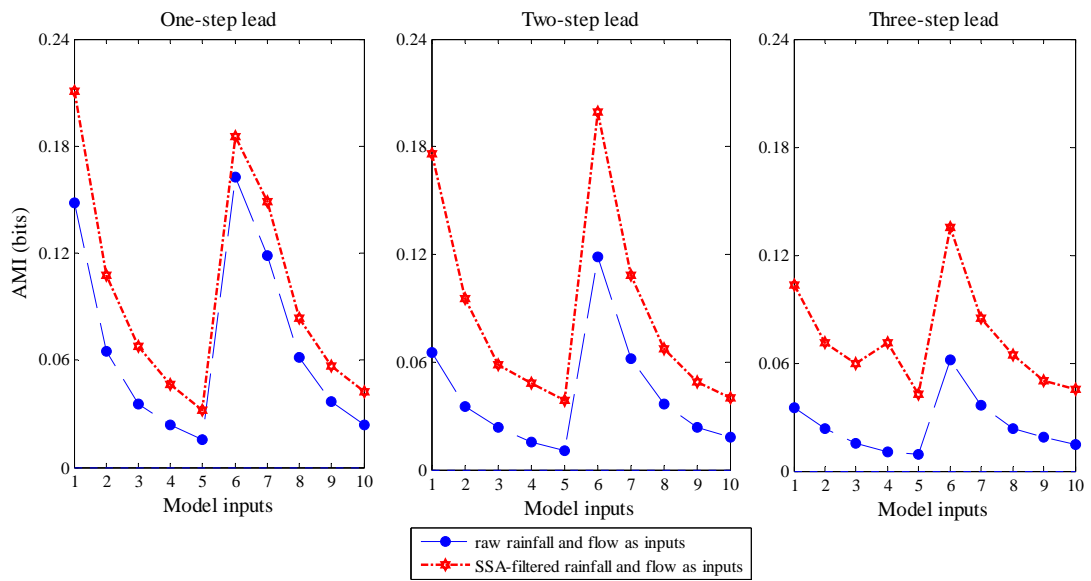
85

Figure 19.



86

87



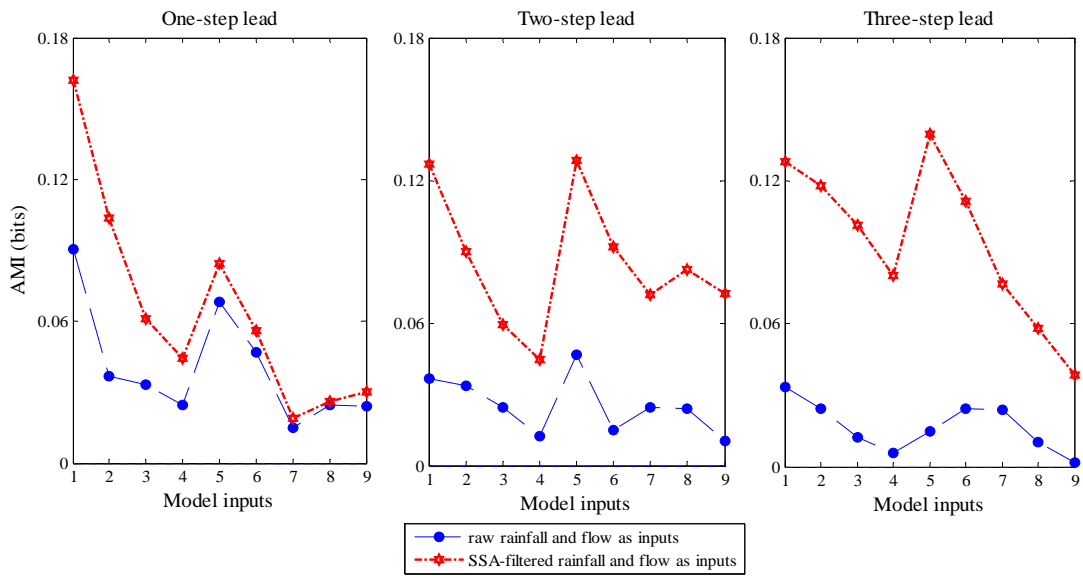
88

89

90

Figure 20.

91



92

93

Figure 21.

1

Table 1. Statistical information on rainfall and streamflow data

Watershed and datasets	Statistical parameters						Watershed area and data period
	$\mu$	$S_x$	$C_v$	$C_s$	$X_{\min}$	$X_{\max}$	
<b>Wuxi</b>							
<i>Rainfall(mm)</i>							
Original data	3.7	10.1	0.36	5.68	0	154	Area: 2 000 km <sup>2</sup>
Training	3.4	8.9	0.39	4.96	0	102	
Cross-validation	3.8	10.9	0.35	6.27	0	147	Data period: Jan., 1988- Dec., 2007
Testing	4.0	11.6	0.35	5.46	0	154	
<i>runoff(m<sup>3</sup>/s)</i>							
Original data	61.9	112.6	0.55	7.20	6	2230	
Training	60.6	95.6	0.63	5.90	8	1530	
Cross-validation	60.7	132.2	0.46	8.35	6	2230	
Testing	66.0	122.1	0.54	6.30	10	1730	
<b>Chongyang</b>							
<i>Rainfall(mm)</i>							
Original data	3.1	8.5	0.4	5.7	0.0	122	Area: 1 700 km <sup>2</sup>
Training	3.5	9.8	0.4	5.7	0.0	122	
Cross-validation	2.9	7.0	0.4	3.9	0.0	48	Data period: Jan., 2004- Dec., 2007
Testing	2.6	7.0	0.4	5.6	0.0	78	
<i>runoff(m<sup>3</sup>/s)</i>							
Original data	39.1	54.8	0.7	6.4	2.1	881	
Training	48.1	70.1	0.7	5.5	6.9	881	
Cross-validation	35.6	33.7	1.1	2.3	4.4	226	
Testing	24.5	25.7	1.0	5.1	2.1	310	

2

3

4

5

Table 2. Comparison of methods to determine mode inputs using ANN

Watershed	Methods	$\tau$	$l_1$	$l_2$	$m$	Effective inputs	Identified ANN	RMSE
<b>Wuxi</b>								
	LCA	1	5	5	10	all	(10-8-1)	41.98
	AMI	1	5	5	10	all	(10-8-1)	41.98
	PMI	1	5	5	10	all	(10-8-1)	41.98
	SLR	1	5	5	10	except for Rt-3	(9-5-1)	40.54
	MOGA	1	5	5	10	Rt, Rt-1, Rt-2, Rt-3, Rt-4, Qt, Qt-1, Qt-4	(8-6-1)	43.23
<b>Chongyang</b>								
	LCA	1	5	4	9	all	(9-9-1)	14.43
	AMI	1	5	4	9	except for Rt	(8-7-1)	14.18
	PMI	1	5	4	9	except for Rt	(8-7-1)	14.18
	SLR	1	5	4	9	except for Rt-1,t-2,t-4	(6-9-1)	13.54
	MOGA	1	5	4	9	Rt, Rt-1, Rt-2, Rt-4, Qt, Qt-2, Qt-3	(7-5-1)	13.57

6

7

8 Table 3. Optimal  $p$  RCs of rainfall and runoff input variables at various forecast  
 9 horizons

Filter model	Prediction horizons	Wuxi		Chongyang	
		Optimal $p$ RCs	RMSE	Optimal $p$ RCs	RMSE
<b>LR-RF</b>					
	1	all RCs	57.13	1 3	25.88
	2	1 2 3 5 <sup>a</sup>	58.37	1 2 6	25.81
	3	1 2 3	74.24	1 2 7	25.49
<b>LR-QF</b>					
	1	1 2 3	35.83	1 2 3	8.92
	2	1 2	55.94	1 2	13.41
	3	1	67.60	1	16.60
<b>ANN-RF</b>					
	1	1 3 4 6 7	49.72	1 3 5 7	18.45
	2	1 2 3 4 5	52.38	1 3	19.11
	3	1 2 3 4	60.01	1 2	21.72
<b>ANN-QF</b>					
	1	1 2 3 4	31.49	1 2 3	11.67
	2	1 2 7	45.39	1 2	14.97
	3	3 7	53.55	1	17.26

10 Note: <sup>a</sup> the numbers of “1, 2, 3, 5” stand for RC, RC2, RC4, and RC5, and RC1 is associated with the  
 11 maximum eigenvalue, RC2 corresponds to the second largest eigenvalue, etc.

12

13

Table 4. R-R Model performances at three prediction horizons in the normal mode

Watershed	Model	RMSE			CE			PI		
		1*	2*	3*	1	2	3	1	2	3
<b>Wuxi</b>										
	LR	49.40	89.40	108.90	0.84	0.46	0.21	0.70	0.51	0.39
	ANN	43.97	87.32	104.94	0.87	0.49	0.26	0.76	0.54	0.43
	MANN	40.44	71.87	86.54	0.89	0.66	0.50	0.80	0.69	0.61
<b>Chongyang</b>										
	LR	19.18	22.74	25.53	0.44	0.22	0.01	0.17	0.29	0.24
	ANN	12.90	25.80	27.81	0.75	0.10	-0.15	0.63	0.10	0.13
	MANN	13.27	26.86	23.96	0.74	-0.07	0.14	0.61	0.03	0.35

\* The number of "1, 2, and 3" denote one-, two-, and three-step-ahead forecasts

14

15

16

17

Table 5. Performances of ANN and MANN in two types of input variables

Watershed	Input variables	Model	RMSE			CE			PI		
			1	2	3	1	2	3	1	2	3
<b>Wuxi</b>											
	<i>Rainfall+Flow</i>										
		ANN	43.97	87.32	104.94	0.87	0.49	0.26	0.76	0.54	0.43
		MANN	40.44	71.87	86.54	0.89	0.66	0.50	0.80	0.69	0.61
	<i>Flow</i>										
		ANN	81.3	104.6	111.5	0.56	0.27	0.17	0.19	0.33	0.36
		MANN	75.7	93.7	97.1	0.62	0.41	0.37	0.30	0.46	0.51
<b>Chongyang</b>											
	<i>Rainfall+Flow</i>										
		ANN	12.90	25.80	27.81	0.75	0.10	-0.15	0.63	0.10	0.13
		MANN	13.27	26.86	23.96	0.74	-0.07	0.14	0.61	0.03	0.35
	<i>Flow</i>										
		ANN	20.3	26.1	27.8	0.38	-0.04	-0.18	0.08	0.06	0.10
		MANN	17.8	22.3	23.4	0.52	0.24	0.17	0.29	0.31	0.36

18

19

20

Table 6. Performances of R-R models in the SSA mode

Watershed	Model	RMSE			CE			PI		
		1	2	3	1	2	3	1	2	3
<b>Wuxi</b>										
	LR-SSA	29.02	44.42	58.34	0.94	0.87	0.77	0.90	0.88	0.82
	ANN-SSA	25.40	27.10	33.96	0.96	0.95	0.92	0.92	0.96	0.94
	MANN-SSA	25.08	26.87	34.05	0.96	0.95	0.92	0.92	0.96	0.94
<b>Chongyang</b>										
	LR-SSA	9.19	13.53	14.61	0.87	0.72	0.68	0.81	0.75	0.75
	ANN-SSA	6.22	7.08	11.12	0.94	0.93	0.82	0.91	0.93	0.86
	MANN-SSA	6.42	8.13	13.14	0.94	0.90	0.74	0.91	0.91	0.80

21

22



23 Table 7. Performances of ANN-SSA and MANN-SSA using two types of input variables

Watershed	Input variables	Model	RMSE			CE			PI		
			1	2	3	1	2	3	1	2	3
<b>Wuxi</b>											
	<i>Rainfall+runoff</i>	ANN-SSA	25.40	27.10	33.96	0.96	0.95	0.92	0.92	0.96	0.94
		MANN-SSA	25.08	26.87	34.05	0.96	0.95	0.92	0.92	0.96	0.94
	<i>runoff</i>	ANN-SSA	31.02	50.64	61.80	0.94	0.83	0.74	0.88	0.84	0.80
		MANN-SSA	26.20	41.02	48.69	0.95	0.89	0.84	0.92	0.90	0.88
<b>Chongyang</b>											
	<i>Rainfall+runoff</i>	ANN-SSA	6.22	7.08	11.12	0.94	0.93	0.82	0.91	0.93	0.86
		MANN-SSA	6.42	8.13	13.14	0.94	0.90	0.74	0.91	0.91	0.80
	<i>runoff</i>	ANN-SSA	7.93	11.15	15.72	0.91	0.81	0.63	0.86	0.83	0.72
		MANN-SSA	7.32	10.19	15.71	0.92	0.84	0.63	0.88	0.86	0.72

24